



January 2013

Development Of Second Generation Rolling Contact Fatigue Tester

Satyam Ulhas Deshmukh

[How does access to this work benefit you? Let us know!](#)

Follow this and additional works at: <https://commons.und.edu/theses>

Recommended Citation

Deshmukh, Satyam Ulhas, "Development Of Second Generation Rolling Contact Fatigue Tester" (2013).
Theses and Dissertations. 1414.
<https://commons.und.edu/theses/1414>

This Thesis is brought to you for free and open access by the Theses, Dissertations, and Senior Projects at UND Scholarly Commons. It has been accepted for inclusion in Theses and Dissertations by an authorized administrator of UND Scholarly Commons. For more information, please contact und.common@library.und.edu.

DEVELOPMENT OF A SECOND GENERATION ROLLING CONTACT
FATIGUE TESTER

By

Satyam U. Deshmukh

Bachelor in Engineering, Pune University, 2009

A Thesis

Submitted to the Graduate Faculty

of the

University of North Dakota

In partial fulfillment of the requirements

For the degree of

Master of Science

Grand Forks, North Dakota

May
2013

This thesis, submitted by Satyam U. Deshmukh in partial fulfillment of the requirements for the Degree of Master of Science from the University of North Dakota, has been read by the Faculty Advisory Committee under whom the work has been done and is hereby approved.

Dr. Marcellin Zahui

Dr. Matthew Cavalli

Dr. George Bibel

This thesis is being submitted by the appointed advisory committee as having met all of the requirements of the Graduate School of the University of North Dakota and is hereby approved.

Dr. Wayne Swisher,
Dean of the Graduate School

Date

PERMISSION

Title Development of a Second Generation Rolling Contact
Fatigue Tester

Department Mechanical Engineering

Degree Master of Science

In presenting this thesis in partial fulfillment of the requirements for a graduate degree from the University of North Dakota, I agree that the library of this University shall make it freely available for inspection. I further agree that the permission for extensive copying for scholarly purposes may be granted by the professor who supervised my thesis work or, in his absence by the Chairperson of the Department or the Dean of the Graduate School. It is understood that any copying or publication or other use of this thesis or part thereof for financial gain shall not be allowed without my written permission. It is also understood that due recognition shall be given to me and to University of North Dakota in any scholarly use which may be made of any material in my thesis.

Satyam Deshmukh

1/24/2013

TABLE OF CONTENTS

LIST OF FIGURES.....	vii
LIST OF TABLES.....	ix
ACKNOWLEDGEMENTS.....	x
ABSTRACT.....	xi
CHAPTER	
I. INTRODUCTION.....	1
1.1 Background.....	2
1.2 Factors Causing Rolling Contact Fatigue Failure.....	4
1.3 Failure Modes of Rolling Contact Fatigue	8
1.4 First Generation RCF tester.....	9
1.5 ZF-RCF Tester.....	12
II. RCF DESIGN.....	14
2.1 Design Requirements.....	14
2.1.1 Ease of Operation.....	15
2.1.2 Speed of Operation.....	16
2.1.3 Loading Capabilities.....	18
2.2 Structure of RCF tester.....	22
2.2.1 Main structure.....	23

2.2.2 Base Structure.....	23
2.2.3 Internal Structure.....	25
2.2.4 Driving Mechanism.....	26
2.2.5 Hydraulics.....	28
2.2.6 Lubrication System.....	30
2.3 Design of Mechanical Elements.....	31
2.3.1 Power Calculations.....	32
2.3.2 Chuck Gripping Force.....	33
2.3.3 Design of the Roller Shafts.....	33
2.3.4 Bolt Selection Calculations.....	36
2.3.5 Chain Length Calculations.....	37
2.4 Stress Analysis of the Tester.....	37
2.5 Fatigue Analysis of Rollers and Roller Shafts.....	40
III. ELECTRONIC COMPONENTS OF THE TESTER.....	44
3.1 Eddy Current Testing Device.....	44
3.2 Data Manipulation System.....	51
3.2.1 Data Storage.....	51
3.2.2 Data Analysis.....	56
IV. TESTING PROCEDURE.....	60
4.1 Test Setup Procedure.....	60
4.2 Testing Conditions and Failure Criteria.....	67

V. RESULTS AND DISCUSSION	69
5.1 RCF Test Bench.....	69
5.2 AISI 8620 specimen.....	70
5.3 Test Procedure and Parameters.....	70
5.4 Results.....	71
VI. CONCLUSIONS AND RECOMMENDATIONS.....	73
APPENDICES.....	74
APPENDIX A.....	75
APPENDIX B.....	88
APPENDIX C.....	93
APPENDIX D.....	96
APPENDIX E.....	99
BIBLIOGRAPHY.....	101

LIST OF FIGURES

Figure	Page
1. General Hertzian stress distribution for contacting cylinders	5
2. Stribeck Curve	6
3. Pitting observed on hardened specimen of first generation RCF tester....	9
4. First generation sliding rolling contact fatigue tester [11].....	11
5. Torque specifications of US Tsubaki sprockets [7].....	18
6. Parameters for Hertzian stress calculations [8]	19
7. Graph of Hertzian stress vs Normal Force.....	21
8. Pro E model of RCF tester.....	23
9. Pro E model of base structure.....	24
10. Pro E model of loading mechanism.....	25
11. Allen-Bradley 10 hp Motor.....	27
12. Motor Controllers.....	28
13. Hydraulic Circuit. A – Hydraulic power unit, B – Pressure Regulator, C – Pressure Guage, D – 3 Way 4 Ports Directional Valve, E,F – Hydraulic Cylinders.....	29
14. Photo showing lubrication system.....	30
15. Photo of Nozzles used to spray lubricant on the specimen.....	31
16. Bending moment diagram of the roller shafts.....	34

17. Schematic Diagram explaining the forces on the bolts.....	36
18. Deformation Analysis of the Tester.....	38
19. Cylinder Mounts with reinforcement.....	39
20. Deformation Analysis of the tester with reinforcement.....	39
21. Stress Analysis of the Tester.....	40
22. Typical S-N curve.....	41
23. Typical Basquin Curve.....	41
24. Fatigue Analysis on Rollers.....	42
25. Fatigue Analysis on Roller Shafts.....	43
26. a) The alternating current flowing through coil generating magnetic field, b) Eddy current induced in the material, c) Change in impedance observed due to a flaw [16].....	46
27. Foester Defectomat EZ 2.828 Eddy Current Detection Device.....	48
28. Diagram showing difference in skin depth between different frequencies, conductivities and permeability while using a eddy current device.....	49
29. Flowchart of failure detection system.....	58
30. Photo showing ECCD system.....	67
31. Pitting observed on Specimen 2.....	72

LIST of TABLES

Table	page
1. Hertzian stress applied to specimens in First generation RCF tester [11]....	11
2. ZF-RCF tester results of various materials [9].....	13
3. Details of conversion factors used for Data Manipulation System.....	52
4. Inputs required for Matlab® Files.....	57
5. Test Conditions.....	70
6. Setting of eddy current instrument.....	71

ACKNOWLEDGEMENTS

I would like to take this opportunity to appreciate University of North Dakota and Advanced Engineering Materials Centre for their efforts in making this project a reality. Without the support and vision of AEM , this project would not have been a possibility. A special thanks Dr. Mike Mann for his financial help.

I would also like to thank the Mechanical Engineering Department of the University of North Dakota for the assistance. I would like to thank Dr. Marcellin Zahui for his immense help and wisdom throughout the project. I would also like to thank Dr. George Bibel and Dr. Matt Cavalli for their guidance.

Gary Dubuque and Jay Evanstad have been a great help during assembly stage of this project. Their help is greatly appreciated. I would like to thank Teri Salwey and Connie Larson for all the immense paperwork that had to be done during the course of this project. A special thanks to Greg Dvorak for his vision of second generation S-RCF tester.

Finally I would like to thank all my family and friends for being there for me and believing in me.

ABSTRACT

Contact fatigue failure has been in research since the early twentieth century. The need for a second generation sliding-rolling contact fatigue tester was proposed by Gregory Dvorak and Dr. Marcellin Zahui. The first generation RCF tester was used for testing super finishing processes for gear surfaces. The second generation RCF tester was funded by the Advanced Engineering Materials lab of University of North Dakota.

Verification of the second generation Rolling Contact Fatigue Tester will be discussed in this thesis including the design details, assembly and testing procedure and to discuss its different parameters. The tester will have the capability of testing hollow specimens using a bobbin eddy current testing probe. This tester will allow a wide range of experiments and is not built for one specific purpose. An eddy current device is used for detecting cracks. The loading force is applied using hydraulic cylinders and a hydraulic power unit. Before testing began, the machine was run for some time at full speed. A lot of minor problems were detected and fixed.

Three specimens of AISI 8620 were tested in this tester. All tests gave results matching with some of the other well-known RCF testers. These tests were performed to evaluate mechanical limits of the tester and to evaluate the software performance of the tester.

CHAPTER I

INTRODUCTION

The idea of a second generation Rolling Contact Fatigue (RCF) tester was proposed by a UND's graduate student Gregory Dvorak who had worked on the first generation RCF tester. Since the first tester was completely manufactured in UND's machine shop, the tolerance and the quality of the finished parts were not up to par. This resulted in higher noise and vibration than expected. There was a need for a new and better tester with ease of operation and better loading capabilities. The University of North Dakota's Advanced Engineering Materials Centre (AEMC) funded the development of a second generation rolling contact fatigue (RCF) test machine to simulate contact fatigue. This machine simulates contact under sliding and rolling conditions to test the effect of surface finishing process. AEMC will use this machine for doing more research on RCF.

The first generation tester was developed by a group called PENTA-X for their senior design project in 2006. One of the members, Gregory Dvorak, completed the construction after graduation and performed preliminary tests in 2008. The design of the second generation RCF began in December 2010. The design process and improvements over the old tester will be discussed in this thesis.

1.1 Background

In any Mechanical Design, failure is inevitable. Failure can be defined as any change in shape, size or material properties of a component or the whole machine or mechanism itself. It is a design engineer's job to ensure that the design does not fail before the prescribed life of the machine or mechanism or a part is over. Success can be achieved by evaluating and recognizing all the potential failure modes possible.

For metals failure can occur through a lot of different modes. The most commonly studied failure mode is excessive deformation or yielding. Other mechanical failure modes are ductile failure, brittle fracture, impact loading, fatigue etc. Almost 50 to 90 percent of the failures are due to fatigue [1]. These include items used daily like tennis raquets, paper clips etc. Fatigue failure is also observed in complex structures like automobile steering linkages, engine connection rods etc.

This thesis concentrates on rolling contact fatigue which is a type of fatigue failure. Fatigue failure is the most common failure mode. A design engineer should always take this into consideration. In materials science, fatigue is the progressive and localized structural damage that occurs when a material is subjected to cyclic loading [2]. The nominal maximum stress values in fatigue failures are less than the ultimate tensile stress limit, and may be below the yield stress limit of the material. Fatigue failure occurs because of cyclic loading. Loads above a specific threshold can cause microscopic cracks on the surface.

These microscopic cracks then result in fracture. Fatigue failure happens over a period of time. Since it is localized it takes place at a specific location and not the whole part. Fatigue failure is also permanent and cannot be reversed.

Components like gears, bearings, rails, and cams are subjected to rolling contact load, thus their major cause of failure is rolling contact fatigue. Rolling Contact Fatigue, or RCF, is defined as crack propagation in the near-surface alternating stress field within the rolling-contact bodies, which eventually leads to material removal [3]. The crack propagation in RCF usually occurs just beneath the surface or at the surface. Studying RCF can help improve the life of the components mentioned above. These components are used widely in many industries such as transportation, manufacturing, etc., thus studying RCF can save a lot of money.

In rolling surfaces, the contact occurs along a line or a point. In these cases the stress developed are high and are called Hertzian stresses. Hertzian contact stresses are the shear stresses developed near the contact points of the two mating parts [4]. The maximum shear stresses occur at some distance below the surface. In repetitive loads the crack initiation will occur at those areas which have hard and brittle inclusions in angular shape.

Just like S-N curves in uniaxial and bending testing, curves can be generated in rolling/sliding contact fatigue tests. Contact fatigue usually results in multi axial compressive stresses unlike uniaxial or bending tests [4].

Slide ratio plays a crucial role in understanding rolling contact fatigue. The slide ratio (SR) is the ratio of velocities of the surfaces rolling against each other. When simulating gear contact, SR plays an important role. If the velocities of the two surfaces are the same we will be observing simple rolling motion.

1.2 Factors Causing Rolling Contact Failure Fatigue

Rolling contact fatigue is the gradual wear and tear that occurs due to high load between two surfaces rolling relative to each other. Extensive research on factors affecting the life of rolling contact fatigue began in the 1990s and gained worldwide attention after the derailment of a train due to broken rail in Hatfield, UK[5][6].

There are two main classes of factors that affect fatigue life of a material. The first one is called operational factors and the second one is called process induced factors. The environmental factors or operational factors consist of stress, lubrication type, lubrication regime, sliding ratio etc. The process induced factors are the abnormalities or the defects that are caused during the manufacturing stage of the material or the part.

Contact force is the most important operational factor that needs to be taken into consideration while studying rolling contact fatigue [4]. The contact force applied between two curved surfaces will result in Hertzian stresses at the point of contact. Hertzian stresses essentially govern the contact fatigue life as far as the forces on the surface go. The higher the applied force, the higher will be the Hertzian stress resulting in lower fatigue life.

Figure 1 shows a general stress distribution of hertzian pressure for two contacting cylinders. The intensity of the stress field at the point of contact is determined by the magnitude of the force. The general parabolic shape for a hertzian stress field can be seen in Figure 1 [4]

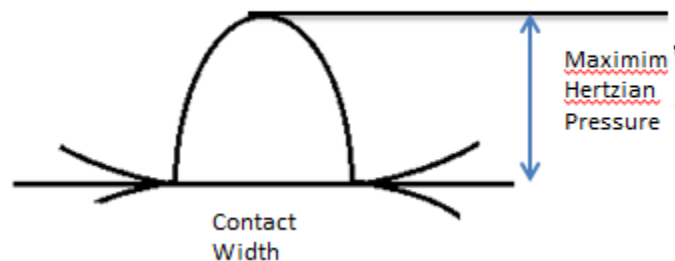


Figure 1 General Hertzian stress distribution for contacting cylinders [4]

To predict the fatigue life of a material in a particular case of uniaxial loading or bending tests, (S-N) curves are produced. Similar curves can be produced when studying rolling contact fatigue [4].

The amount of lubrication supplied should be taken into consideration too, since it will affect the part's fatigue life. There are three types of surface lubrication: Hydrodynamic or full film, boundary, and mixed film and boundary lubrication. Figure 2 shows a curve relating coefficient of friction as a function of process related parameter [5]. The process related parameter is the product of viscosity of the lubrication and speed divided by contact pressure. The surface asperities do not protrude beyond the lubrication in full film lubrication and will not touch the mating surface. In boundary lubrication, there is a thin layer of lubrication present and the load is transferred between the contacting asperities.

The assumption in mixed mode is that load is transferred by both the film and the surfaces [5].

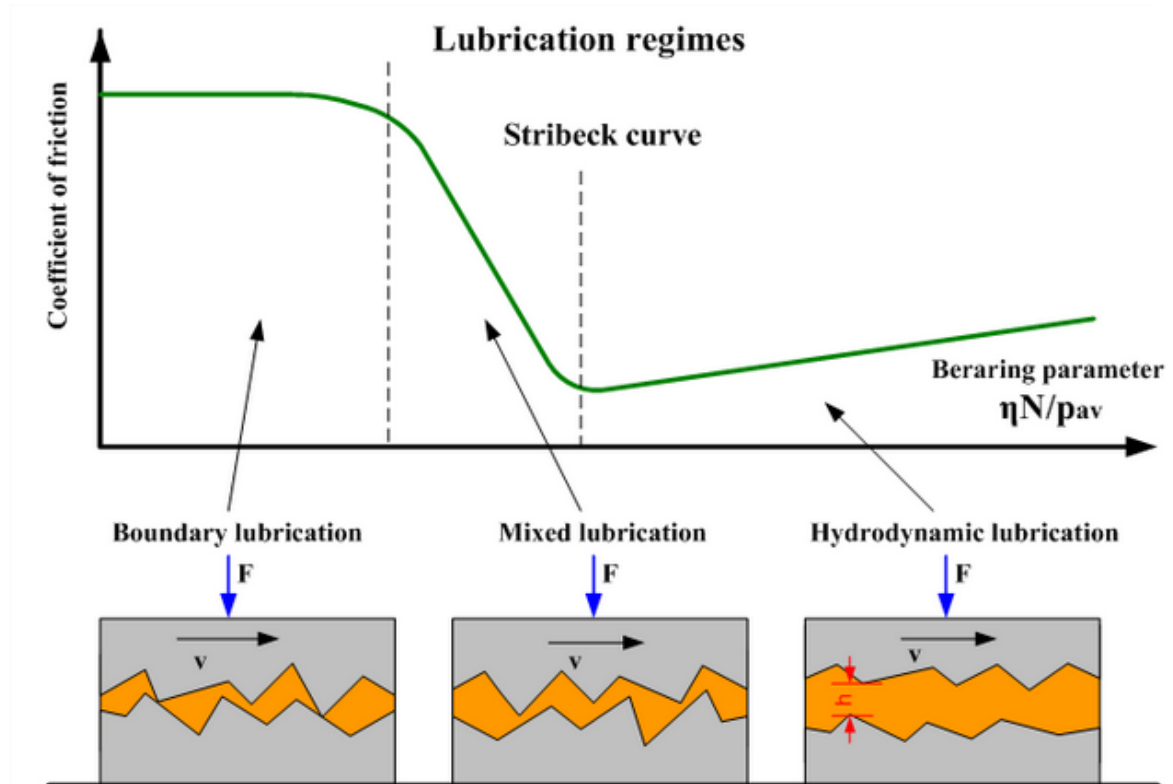


Figure 2 Stribeck Curve [5]

Stribeck curve can give a general idea of heat generated in the surface by friction by drop in the lubricant viscosity and the process parameter [5]. As seen in the Figure 2, decrease of the process parameter in mixed mode lubrication will increase the coefficient friction and subsequently surface temperature. Hence mixed mode lubrication is unstable. Whereas, in full film lubrication, increase of process parameter due to temperature rise will cause the coefficient of friction to drop. The system will correct itself. Thus this is a stable mode of lubrication [5].

Even though surface temperature plays an important role in affecting fatigue life, it is the hardest variable to control. Low temperature will make ductile material more brittle. Any cracks present will propagate more rapidly in this case. High surface temperature caused by friction between mating parts will often reduce the stiffness of materials resulting in weakening between the crystals [6].

The non-environmental factors or process-induced factors are another class of factors affecting fatigue life of parts. The most studied process-induced factor is the surface roughness. To improve the fatigue strength of parts, surfaces can be finely superfinished. Finely finishing the surfaces can have a counterproductive result as well. Grinding operations may introduce high tensile stresses and help fatigue failure. In a similar manner, machine polishing by using abrasives will often generate enough heat to induce serious surface tension. A high roughness surface may prevent the two rolling surfaces from welding but it does cause high variations in the pressure distribution, resulting in localized plastic deformation and crack initiation [4].

Defects in the material that reduce microstructure purity can reduce fatigue strength as these soft spots act as crack nucleation sites. The main effects of microstructure defects are observed in the low stress intensity regime [4]. Heat treatment to increase surface hardness will increase the fatigue life but a poor job during this process can result in higher amount of impurities. Casting of parts will result in porosity. Pores are effective crack nucleation sites. New casting technologies like squeeze casting will tend to eliminate the porosity [4].

In order to keep machining costs at minimum for operations like turning, milling and other machining operations, cutting tools must often take deep cuts at high feed rates. These processes can often result in large internal stresses so deep in the material that finish machining or grinding will not remove the stressed material [4]. In addition, the finishing operation will induce more stresses [4].

1.3 Failure Modes of Rolling Contact Fatigue

The most common failure mode in contact fatigue is pitting. Most operations like grinding, tempering or honing will leave compressive stresses on the surface and tensile residual stresses in the subsurface. In contact fatigue, as discussed earlier, cracks will initiate at crack nucleation sites [3]. Shear stress is usually produced in the subsurface of the rolling bodies because of the contact geometry and the motion. The plastic strain will build up until a crack is initiated. This crack will propagate until a pit is formed due to residual stresses in the material discussed earlier. This pitting will cause friction between the bodies giving rise to noise, surface temperature, rough running and, eventually, failure [3].

Figure 3 below shows on a specimen used in first generation RCF tester. Pitting can be observed on this specimen.



Figure 3 Pitting observed on hardened specimen of first generation RCF tester

The two types of failure modes of contact fatigue are surface-origin (S-O) failure and subsurface-origin (SS-O) failure [3]. The two types of surface origin failure in contact fatigue are Macropits and Micropits. Macropits have large asperities whereas Micropits have small asperities. Joining of more and more Micropits will give rise to Macropits. Inclusion originated Macropits occur at location where there are defects and impurity inclusions in the bulk material. Failure originating at the interface of the case/core interface where the hardness is lower than the Hertzian stress is called as subcase failure [3].

1.4 First Generation RCF Tester

The first tester was developed with taking two things into considerations, first the loading capabilities and second, the time taken for completing one experiment.

The loading requirement for the specimen was based on the 2.1 GPa of Hertzian stress required to fail the specimen of 1.5 inch in diameter [10] for this, two pneumatic cylinders were used. Both cylinders were aluminum tie rod cylinders each with 4.5 inch bore and stroke of 8 inches with maximum allowable pressure of 250 psi. For the second requirement, the conditions were set to complete 30 million load cycles in 48 hours. There are two ways to achieve these, one by increasing the number of contact points or by increasing the rotational speed of the specimen. The motor speed was set at 3500 rpm since the gears that were used could not handle the higher speed and torque. And to reduce the time, three contact points were used.

The first generation RCF tester had three main components. The main structure, which included the base plate, legs, rollers, specimens, gears pneumatics etc. The second component included the lubrication system. The third component included the failure detection system.

Three rollers were used in the first generation RCF tester. The rollers and the specimen were driven by different motors, thus giving the freedom to test sliding contact. The test specimen used in this tester was a cylinder with tapering ends. Rolling contact was tested by keeping the two motors at same speed. And sliding contact was tested by using different motor speeds, thus simulating gear contact.



Figure 4 First generation sliding rolling contact fatigue tester [10]

The material tested in the first generation RCF tester was AISI 8620, since it is a common gear material and fatigue data on it is available. The short cylindrical test specimens were heat treated to 58 to 62 HRC. Three specimens were tested in tolling condition under different pressure. A thin layer of lubricant was sprayed onto the surface before performing the tests. The sample specimen was tested to observe pitting and determine failure criteria.

Table 1 Hertzian stress applied to specimens in First generation RCF Tester [11]

Specimen	Sample	1	2
Average cylinder pressure (psi)	82	63	66
Max. Hertzian stress (GPA)	2.39	2.08	2.13
Cycles to failure in millions	8.64	20	6.26

For the failure criteria for the first generation tester, a voltage increase of .15 was set as benchmark. Since the sample specimen showed considerable pitting. The properties measured of these failed samples were roughness, microstructure analysis and hardness value. As far as the roughness goes Ra values of the rollers were better than those of the specimen as predicted. Therefore in the second generation tester the rollers are kept considerably larger than the specimen.

The hardness of the specimen also showed considerable drop. Hardness was measured at 15 mm intervals on the specimen. Measurements were stopped when the effective hardness value of 50 HRC was reached. Microstructure analysis was done on the specimen by examining them under a microscope, 20 microns from the edge. The amount of retained austenite and other non-transformed products was found out to be 15.13 percent. Visible damage and pitting was also observed in the specimens as seen in figure 7 [1].

1.5 ZF-RCF tester

ZF-RCF tester is also considered for designing the second generation RCF tester. The ZF-RCF tester is a very well-known tester and data from this tester is easily available. The first ZF-RCF tester was developed and tested in Germany, the second tester was created at V-Tech International in West Bend, Wisconsin. This tester uses three rollers just like the first generation RCF tester [7]. The ZF-RCF tester can turn the specimen at 3600 rpm [7]. Table 2 gives the results of

some of the specimens tested by Gottfried Hoffmann and James A. Rice using this tester in 2004 [7]. Pitting was observed on all the specimens tested [7].

Table 2 ZF-RCF tester results of various materials [9].

Material	Hertzian stress (GPa)	Load cycles to first crack (10^6)	Load cycles to final failure(10^6)
AISI 5120	2.1	12.1	14.0
AISI 8620	2.1	15.5	20.7
AISI 1060	2.1	4.3	6.2
AISI 4150	2.1	6.7	7.5

CHAPTER II

RCF Design

In this chapter various design challenges faced in developing the second generation RCF tester will be discussed. The design of first generation tester was taken into consideration and the overall design was improved with keeping some of its parts the same like the motors and electronic components. The design of the second generation RCF tester began Dec 2010. In Chapter I various factors were discussed that affect a material contact fatigue life like lubrication regime, hertzian stress etc. All these factors were taken into consideration while designing the tester. The most important factor was manufacturability of the components to keep the costs low. This chapter will give a in depth analysis of various design steps taken.

2.1 Design Requirements

The three design requirements considered for the tester were

1. Ease of operation,
2. Speed of operation,
3. Loading capability,

2.1.1 Ease of Operation

A big issue in the first generation RCF tester was disassembling and assembling procedure before and after each experiment. Both motors had to be removed and reattached before and after every test to allow removing and placing the specimen. This procedure requires two people as the motors are heavy. It is also extremely time consuming as the motors need to be perfectly aligned every time they are mounted back on the machine. Even the roller shafts had to be removed before each test which required taking apart the machine almost completely.

To address this issue the machine was redesigned completely. Instead of 3 rollers only 2 rollers were used. The top roller was eliminated so that the specimen can be accessed from the top. The roller shaft also had to be unconstrained along the radial axis of rotation. To solve this problem, instead of gears, a chain-sprocket mechanism was used. This would allow the user to push back the roller shafts so that the specimen can be removed with ease. This new design eliminates the need to remove the motors after each test and also eliminates the need to remove the roller shafts. The only part that needs to be removed is the cover of the oil tank. Details of assembling and disassembling procedure are discussed in Chapter III and Appendix B.

2.1.2 Speed of Operation

The second design requirement that will be discussed in this chapter will be the speed of operation. The faster the specimen rotates, lesser time will be required to complete a test. More contact points will also mean that less time will be needed per test. Taken into account load cycles from ZR-RCF tester, we have a datum to go about the problem of speed of operation [7].

As discussed in Chapter I, it takes almost 20.7 million cycles to fail AISI 8620, two contact points were provided in second generation RCF tester. It was decided that it should not take more than 2 days to test a specimen.

$$\omega_s = \frac{N}{2 \cdot t} \quad (1)$$

where ω_s is the speed of the specimen (rpm), N is the number of cycles to failure, and t is the time in minutes to failure. The factor of two in the above equation represents the two contact points in the tester. Taking the 20.7 million cycles and 2 contact points the speed of operation was set at 3500 rpm. The motors used for providing the rotational speed were the same used by the first generation tester. The motors were 10hp motors. Since the tester uses sprocket and chain mechanism for providing rotation, selection of sprocket was made from US Tsubaki catalog [11].

Since the diameters of the rollers and the specimen are different, the rpm of the two motors will be different. In pure rolling the linear velocities of the specimen and roller will have to be same.

$$V_s = V_r \quad (2)$$

Here V_s and V_r are the velocities of the specimen and rollers respectively. The rollers have a radius of 2.75 inches whereas the specimen has a radius of 1 inches. Since the rotational speed is a function of radius, the rotational speed of the rollers will be 1300rpm considering the specimen is rotated at 3500rpm. Therefore the drive shaft is rotated at 1300 rpm. This speed is more than the motors are capable of. Hence it is safe to say that we can run the experiment at more than 3500 rpm, the only other parameter that will decide the speed of the operation is the horsepower rating of the motors. This will be discussed later in this Chapter.

The sprocket diameter could not be more than 5 inches because of the distance between the drive shaft and the roller shaft. Keeping these two points in mind RS 60, triple strand sprocket 17 teeth was selected. According to the graph in Figure 5, the maximum speed of the sprocket used should not exceed 2,000rpm for transmitting 10 hp [11].

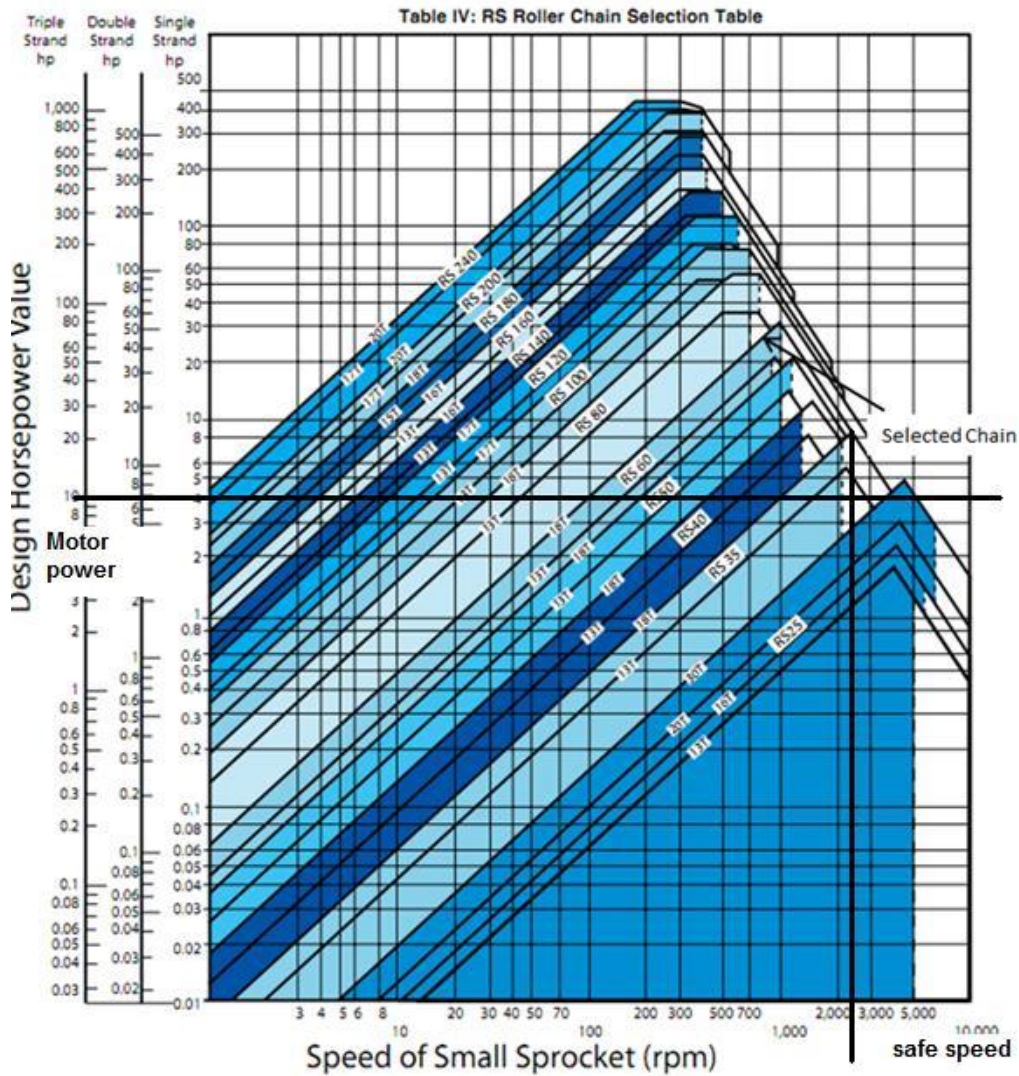


Figure 5 Torque specifications of US Tsubaki sprockets [7]

The third design requirement for the tester was its loading capability. The loading capabilities of the tester are discussed in the next segment.

2.1.3 Loading Capabilities

The final design requirement of the tester was its loading capabilities. The most important parameter to be considered in contact mechanics of gears, bearing and other components that go through contact fatigue is the Hertzian

stress. This section will give a brief idea about why studying Hertzian stress is important and how this design requirement was met.

When two curved surfaces are in contact and sliding or rolling against each other, the stresses developed near the point of contact are known as hertzian stresses. In the first generation tester the Hertzian stresses achieved were close to 2.1 GPa. In the second generation tester the Hertzian stress requirement was increased to 3 GPa. Calculations for the Hertzian stress will be different for different cases. Formulae for calculating Hertzian stress are different for contact between two spheres, contact between two cylinders with unparallel axes, and many other cases. The case that we are dealing with is two cylinders with parallel axis. The hertzian stresses can be approximated if the contact length (L), the radial force applied (F_r), and the dimensions of the rolling surfaces are known [9].

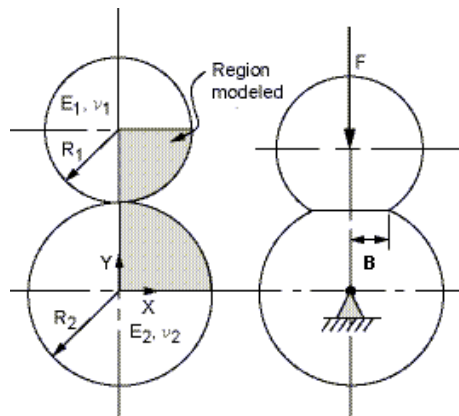


Figure 6 Parameters for Hertzian stress calculations [8]

$$P_{Hz} = 4 \cdot \frac{F_r}{L \cdot \pi \cdot B} \quad (3)[9]$$

Here P_{Hz} is the hertzian stress. The size of the specimen for preliminary consideration was taken to be 2 inches in diameter and that of the rollers was 5.5

inches in diameter. The only unknown in the above equation is the contact width B. As seen in Figure 6 contact width is the width of the contact line between the two cylinders. To account for the size difference between the two contacting surfaces the effective radius has to be calculated [9].

$$R = \frac{R_1 \cdot R_2}{R_1 + R_2} \quad (4)[9]$$

Just like the radius correction, the stiffness correction has to be calculated using the Young's moduli and Poisson's ratios of the two respective surfaces. The radius correction factor and the young's moduli correction are used when the radius and the material properties of the two cylinders are different [9]. The following equation shows how to calculate stiffness correction (K_i) for a surface [9].

$$K_i = \frac{1 - \nu_i^2}{\pi \cdot E} \quad (5)[9]$$

And the contact width is calculated by

$$B = \sqrt{\frac{(16 \cdot F_r \cdot (K_1 + K_2) \cdot R)}{L}} \quad (6)[9]$$

The specimen used in the first tester had a diameter of 1.5 inch. For the second generation the specimen size was increased to 2 inches. To calculate the maximum force required, Hertzian stress of 3 GPa for a specimen of 2 inches and a roller of 5.50 inches with contact length of .5 inches and material AISI 8620 were considered. Maximum force of 57.5 kN was required. Since the majority of the tests carried out were at hertzian stress of 2.5 GPa, the RCF tester will carry

out tests at 2.5 GPa. For 2.5 GPa the radial force needed is calculated to be at 20 kN to 45 kN. The figure below shows two specimens taken into consideration. The first one with 1.5 inch diameter and contact length of .25 inches and the second one with 2 inches in diameter and .5 inches of contact length. Figure 10 is graph of hertzian stress vs normal force required.

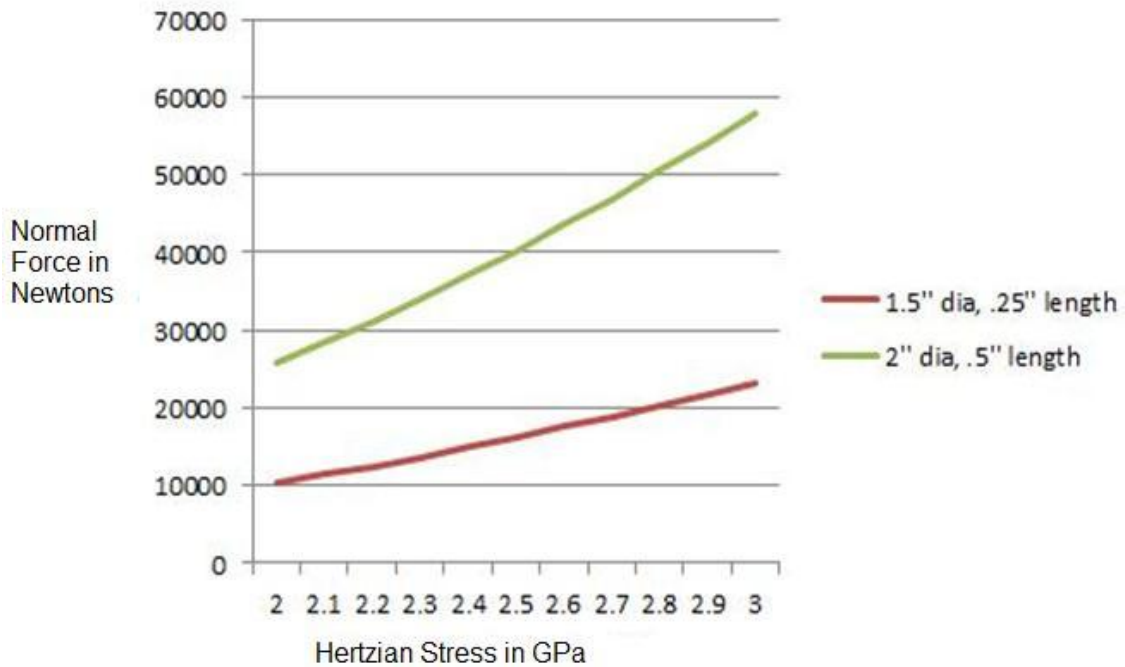


Figure 7 Graph of Hertzian stress vs Normal Force

The normal force will affect the power required to turn the shafts. This normal force will restrict the rotation of shafts. Thus, the power required will more as you will increase with the normal force. The power calculations for the motors are discussed in this Chapter.

Since the force required was much higher than the force required for the first generation tester, hydraulics were taken into consideration instead of

pneumatics. After taking a lot of hydraulic cylinders into consideration, Parker CHD compact hydraulic cylinders were selected because of its compact size and flexibility of manufacturer. Two cylinders with 80 mm bore and stroke of 6 mm was selected. This cylinder is capable of force up to 104 kN which is three and half times more than required [12]. The first reason for selecting a cylinder with bigger bore was to make operating it at a lower pressure possible to avoid leakage problems. And also, if needed in the future, the same cylinders could be used to test at higher loads.

A Haldex Barnes power unit was selected to provide pressure for the cylinders. This power unit is capable of supplying oil at a pressure of up to 3000psi or 107KN [13]. This met our requirements.

2.2 Structure of RCF tester

The RCF tester's design began in December 2010. The tester was manufactured and assembled between December 2011 and January 2012 by Satyam Deshmukh and Dr. Marcellin Zahui.

A robust tester will effectively control and monitor several factors like load, lubrication regime, slide ratio, etc. which were discussed in Chapter 1. The quality of the results will depend on accurately controlling the operational and environmental conditions.

The RCF tester had two main components, the main structure and the failure detection system.

2.2.1 Main structure

The main structure consists of base structure, the internal structure, the driving mechanism and the loading mechanism. The electronics such as motor controllers, eddy current testing system, and the computer are not included in the main structure.

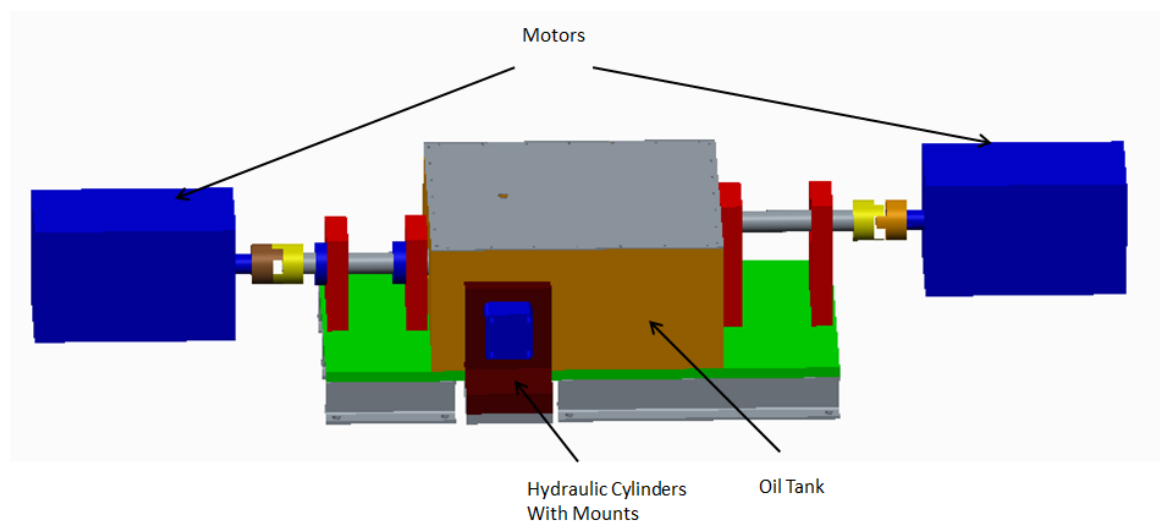


Figure 8 Pro E model of RCF tester

2.2.2 Base structure

The base structure is made of a base plate and 4 I-beam legs. Everything except the motors is connected to the base plate. The base plate is a 1 inch thick steel plate. The base plate is placed on top of 4 standard I-beams of size W 4X13.

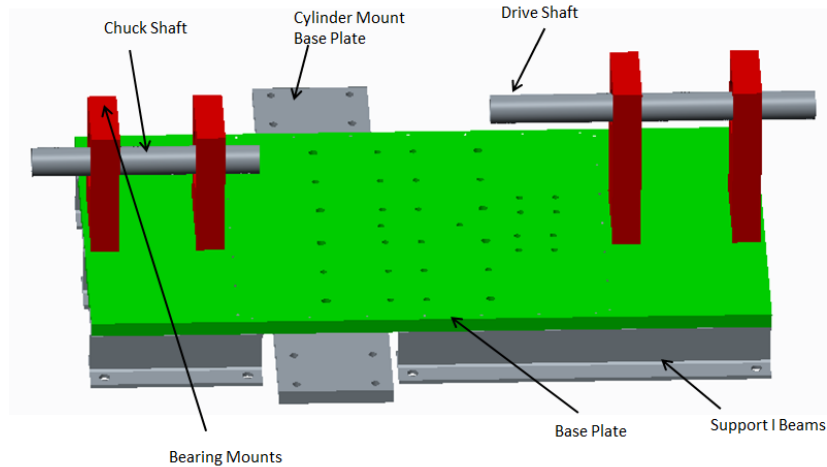


Figure 9 Pro E model of base structure

The base structure also includes the driving shaft and the chuck shaft. Both the shafts are made from AISI 1144 steel. AISI 1144 steel is stress proof and is most suitable for high torque applications like in our case [14]. Stress proof steel is cold rolled through a patented die by Niagara Lasalle steel products. This procedure relieves stress. This results in increased manufacturability and increased strength. Design of these shafts will be discussed in detail in next segment in this chapter. Also included in the base structure are the four bearing mounts for these shafts. The base plate for the hydraulic cylinders also belongs to the base structure. Once the base structure is assembled, there would be no need to flip the base plate and the base structure can be anchored to the ground without the need of moving it to assemble all the other components. The entire assembly procedure will be discussed in detail in Chapter III.

2.2.3 Internal Structure

The internal structure is the core of the RCF tester. The internal structure mainly consists of the part that is to be tested, or the specimen, and two rollers providing two points of contact. The specimen can be from 1.1 inches to 2. inches in diameter and 4.5 inches in length. The rollers are 5.5 inches in diameter and .5 inch thick. Bigger rollers ensure that the failure of the rollers occur after the failure of the specimen. Since the roller is almost 2.5 times bigger than the specimen, one load cycle of the roller equals to 5 load cycles of the specimen.

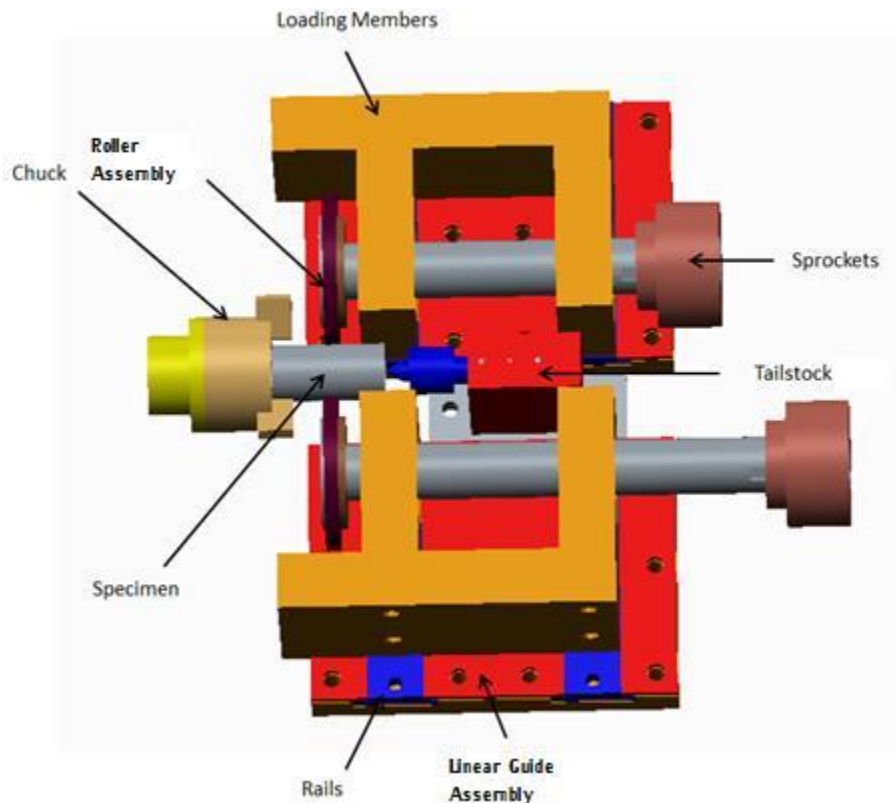


Figure 10 Pro E model of loading mechanism

The specimen is held by a chuck. The chuck shaft is rotated using a 10 hp motor. The rollers are rotated using another 10 hp motor with the help of sprocket chain mechanism. The roller assembly needs to move in the radial direction so that it is easy to load the specimen. Therefore the rollers are connected to a guide mechanism. The loading mechanism provides the rollers with the necessary movement. The loading mechanism consists of loading bearing mounts, guides and the guide sliders. Loading bearing mounts are made from standard 2X6 blocks. They are connected to the guide sliders using 6 9/16 UNC bolts. The guide supports and the rail had to be heat treated for maximum resistance against wear and tear since the rails will be rubbing against guide supports. The guide support had to be made in 6 different pieces to bring down the cost of manufacturing. A live center is provided to support the 4 inch specimen.

2.2.4 Driving Mechanism

The motors that are being used are Allen-Bradley® CM203-NV01035AXZHA-547. The motors operate on 230V or 460V three phase AC power. Encoders are attached to the motors allowing each motor to be precisely controlled. The maximum speed that can be attained with these 10 hp motors is 3550 rpm. The motor drives the two rollers through a sprocket-chain mechanism. As discussed earlier the sprockets are standard RS 80 sprockets from US Tsubaki. Each of these sprockets has 17 teeth, and has three rows of teeth.

The shafts on the motors are 1.875 inches in diameter and the shafts in the internal structure and the base structure are 2 inches in diameter. To connect the two shafts, spider couplers were used. Spider couplers allow for an angular misalignment of 1° and a parallel misalignment of .015 inches [16].

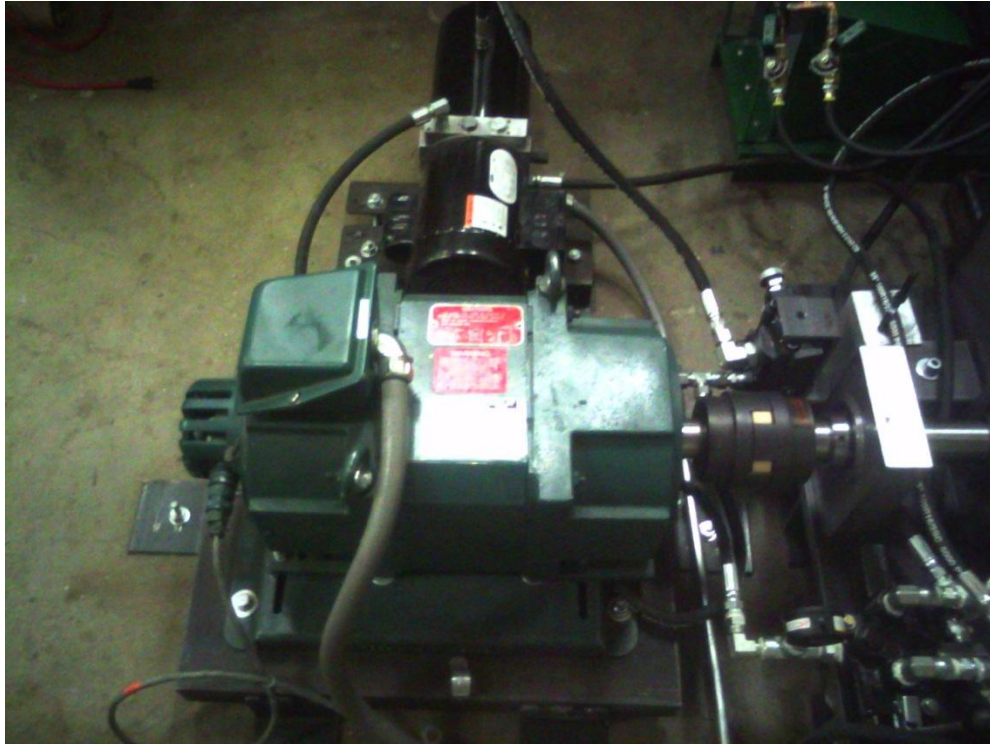


Figure 11 Allen-Bradley 10 hp Motor

Two different motor controllers are used to control the two motors. Using a master-slave setup, the specimen is controlled by the master controller and the rollers are controlled by slave controller. The master controller is the Power Flex 70 and the slave controller is the Power Flex 700S. These motor controllers have Volts per Hertz control or V/Hz control, flux vector control and sensorless vector control. There are many other types of drives available like voltage-source inverter, current-source inverter, six step inverters, load commutated inverters

etc. V/Hz control is essential since the motors that we are using are AC motors. In variable torque applications, AC motors require their output to be adjusted in a linear V/Hz relationship. V/Hz control is best suited for high speed, high performance application like this one.



Figure 12 Motor Controllers

2.2.5 Hydraulics

The rollers are displaced using two Parker-Hannifin hydraulic cylinders capable of providing force up to 104 kN as discussed earlier. A Haldex Barnes power unit was used to provide with the required pressure. The power unit purchased is capable of providing a maximum pressure of 3000 psi. To

synchronize both the cylinders a manual directional valve was used. The force required to test the steel specimens was calculated to be 60 kN.

The pressure needed to provide a force of 60 kN can be calculated using simple force pressure relationship. 2000 psi of pressure is needed to provide the necessary force of 60 kN for the 80mm bore parker cylinders used. A pressure reducing valve from Parker, part number R4V065B310A1, was selected to lower the pressure in the system. This pressure valve is capable of regulating pressure from 100 psi to 3045 psi. An open centre directional valve was selected. The valve has 4 ports and 3 positions. An open Centre directional valve was necessary to reverse the direction of pressure. After the experiment is carried out, it would be necessary to bring back the cylinders to original position.

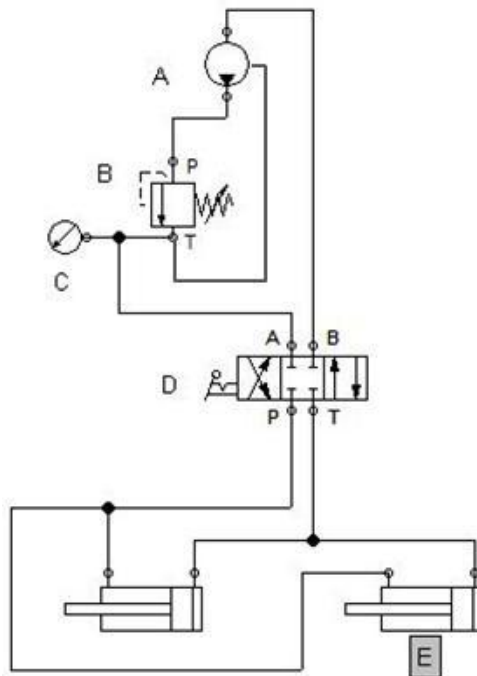


Figure 13 Hydraulic circuit. A – Hydraulic power unit B – Pressure Regulator, C – Pressure Gauge, D – 3 Way, 4 Ports Directional Valve, E,F – Hydraulic Cylinders.

2.2.6 Lubrication system

The lubrication system was installed in the RCF tester since there were leaks in the oil tank. Even though the leaks were repaired, it was decided to use a lubrication system just in case there were more leaks in the future. The lubrication system provides with mixed lubrication regime during testing.

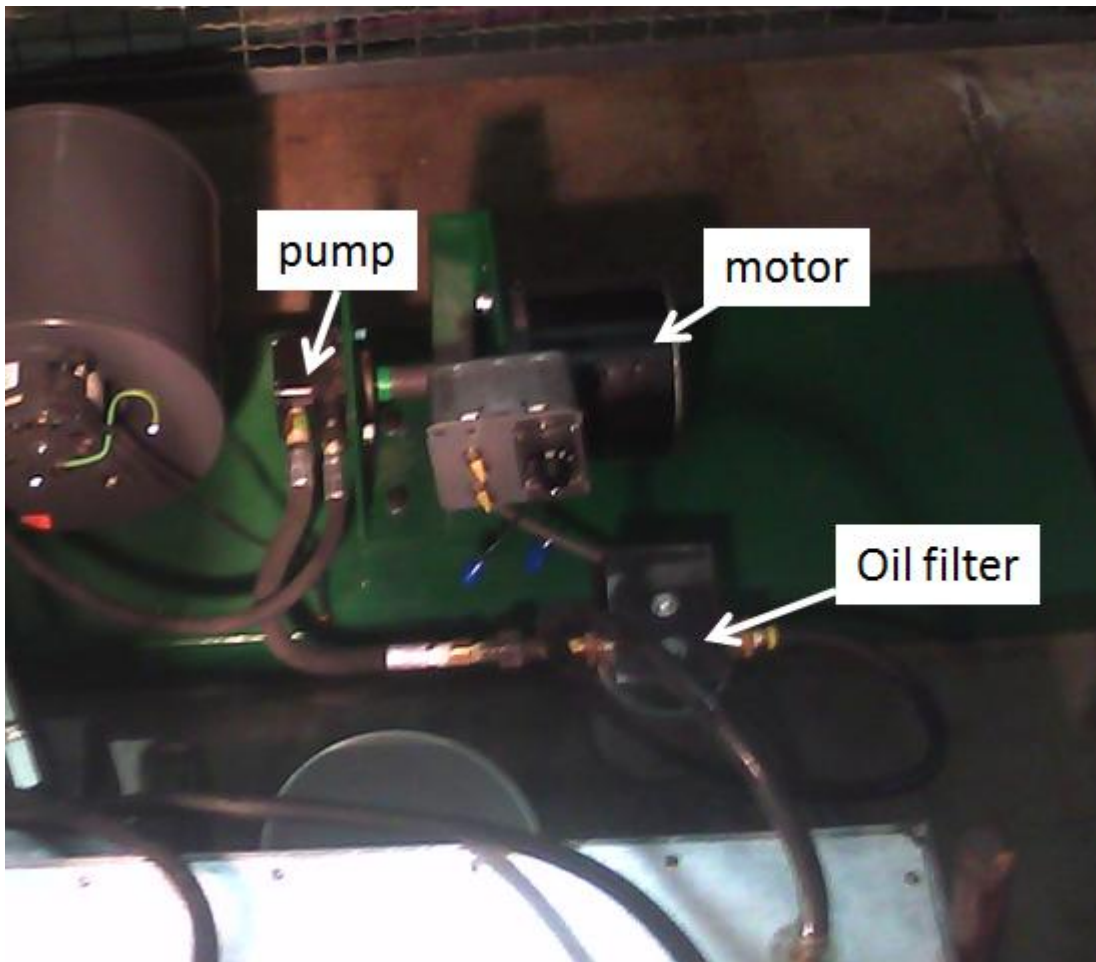


Figure 14 Photo showing lubrication system

Two nozzles were used to provide the necessary film of Dextron 3 transmission fluid on the specimen and rollers. The system consisted of a simple motor-pump

assembly. A filter was also used to remove debris from the wear and tear that occurs during testing.

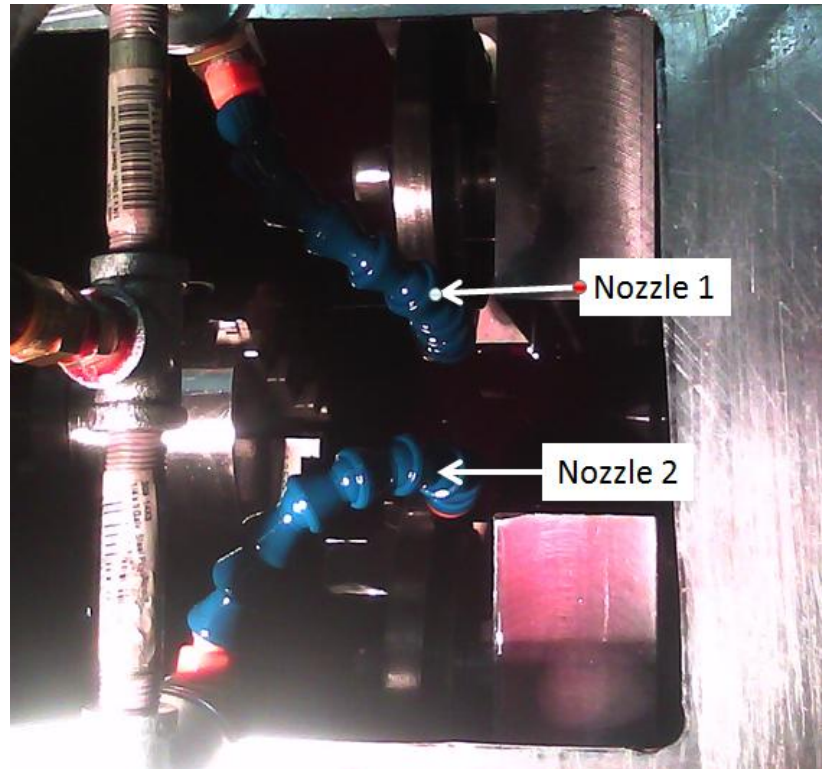


Figure 15 Photo of Nozzles used to spray lubricant on the specimen

2.3 Design of Mechanical Elements

In this section, design of various machine elements will be discussed. We will be going through a brief discussion and going through calculations which will help us understand why some of the parts were selected.

2.3.1 Power Calculations

The normal force (F_r) required to achieve Hertzian stress can be calculated by equation 2. The tangential force F_t , can be calculated using the following equations 7 and 8.

$$F_t = F_r \cdot \frac{f}{r} \quad (7)[15]$$

$$F_t = F_r \cdot \mu_k \frac{f}{r} \quad (8)[15]$$

In these equations f is the coefficient of rolling friction, r is the radius of the specimen and μ_k is the coefficient of friction under sliding conditions. μ_k is the kinetic friction and for surface with relative motion, like in sliding conditions [15]. The coefficient of rolling friction for steel on steel is 0.0005m [15] and the maximum radial force taken into consideration is 60 kN. From the tangential force, the torque required to be provided by the motors and the power required can be calculated using equation 8.

$$T = F_t \cdot r \quad (9)[15]$$

The torque calculated is 1524N-m considering radius of 1 inch. Power required, P to rotate the specimen can be calculated using equation 9.

$$P = C_p \cdot T \cdot \omega \quad (10)[15]$$

Here C_p is the number of contact points and ω is the speed of the specimen (rpm). From the above calculations we reached the conclusion that using two 10 hp motors, a 2.5 GPa hertzian stress test can be carried out at 3500rpm.

2.3.2 Chuck Gripping Force

The tangential force caused due to friction between the steel roller and specimen comes at 1.25 kN. And the torque at 3500 rpm, is calculated at 47 Nm. Since the tangential force is 1.25 kN, chuck type F+ 125 was selected. Chuck type F+125 has maximum gripping force of 37 kN and is the smallest chuck manufactured by buck chuck company [17]. Since maximum gripping force of the selected chuck is greater than the tangential force, chuck type F+125 was selected.

2.3.3 Design of the roller shafts

Four shafts were needed in the whole machine. It was important that all the shafts be of same size and that size be standard. It was important for the shaft size to be standard so that the bearings and spider couplers be easily available and interchangeable. Figure 16 shows the free body diagram (FBD) with loads on the small roller shaft and long roller shaft.

The machine was run using two 10 hp motor. The specimen speed was set at 3500 rpm. Considering the ratio of the radii of the specimen and the rollers, roller shaft speed would be 1200 rpm. Considering this the torque on the roller shafts can be calculated by

$$T = \frac{HP}{rpm} \cdot 5252 \quad (11)[19]$$

The torque on shafts is calculated to be 43.7 lb.ft. or 59.25 N-m. The 60 kN of force (F_r) used to provide Hertzian stress of 3 GPa also needs to be taken into

consideration. The length of the shaft outside the bearing is kept only 1.75 inches. For calculating reaction forces in the bearings, let us take moment about B and C.

$$\sum M_B = L_{AB} \cdot F_r + L_{BC} \cdot F_C = 0 \quad (12)[19]$$

$$\sum M_C = L_{AC} \cdot F_r - L_{BC} \cdot F_B = 0 \quad (13)[19]$$

Solving the above two equations we get $F_B = 75 \text{ kN}$ and $F_C = 15 \text{ kN}$.

Figure 16 shows the bending moment diagram of the shaft

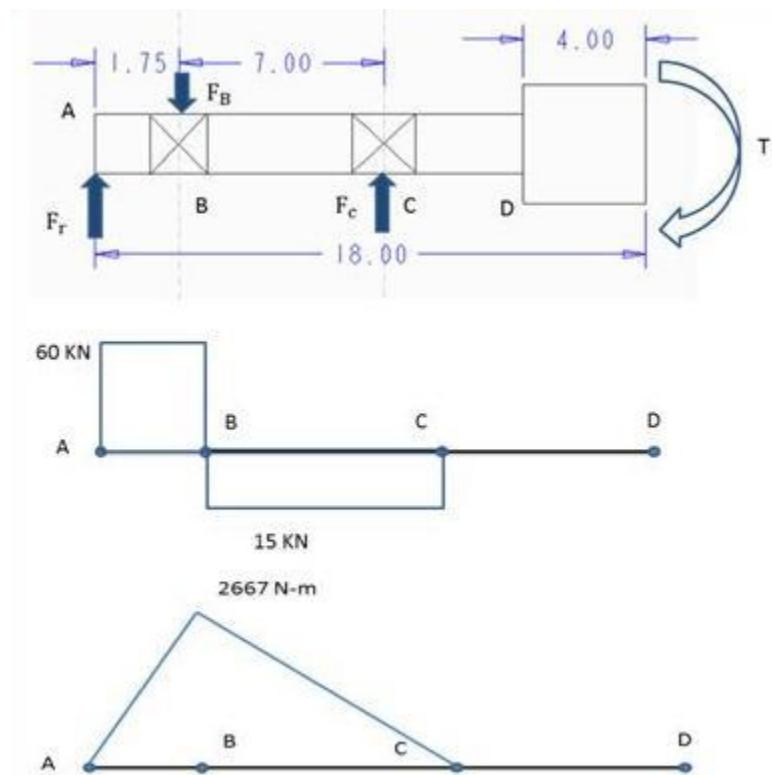


Figure 16 Bending moment diagram of the roller shafts

Using this formula the moment experienced is 2667N-m. With the moment and torque known, the bending and shear stress can be calculated.

$$\sigma = \frac{M}{I} \cdot r = \frac{M}{(\pi \cdot d^4 / 64)} \cdot \frac{d}{2} \quad (14)[19]$$

$$\tau = \frac{T}{J} \cdot r = \frac{T}{(\pi \cdot d^4 / 32)} \cdot \frac{d}{2} \quad (15)[19]$$

Maximum allowable shear stress can be calculated by

$$\tau_{\max} = \sqrt{\left(\frac{\tau}{2}\right)^2 + \sigma^2} \quad (16)[19]$$

Solving the above equations we get

$$T_e = \sqrt{M^2 + T^2} = \frac{\pi \tau \cdot d^3}{16} \quad (17)[19]$$

This equation can be solved for r. AISI 1144 material was selected for the shafts. The tensile strength of this material is 385 MPa [19]. It is cold rolled and stress proof. The stress is relieved by using a patented die. This material has very good toughness and excellent machinability. Hence this material is useful in high torque, high speed applications. Using these equations, acceptable diameters of the shafts were found out to be .4 inches. Using a factor of safety of 2 for keyways and factor of safety of 2 considering the material is delivered by a reliable source, shaft diameter of 1.5 inches was considered. Since the motor shaft was 1.875 inches in diameter, shafts of 2 inches were selected to keep the keyways on both shafts the same.

2.3.4 Bolt Selection Calculations

Considering the 60 kN (or 13488 lbf) force on the loading mechanism and 8 bolts used to carry the force, we can select bolt size using energy distortion theorem.

$$S_{sy} = 0.58 \cdot S_y \quad \mathbf{18[19]}$$

Where S_{sy} and S_y are shear yield strength and maximum shear strength.

Allowable force in these shear planes is calculated by

$$F = 2 \cdot S_{sy} \cdot A \quad \mathbf{19[19]}$$

Where A is the tensile stress area of the bolt.

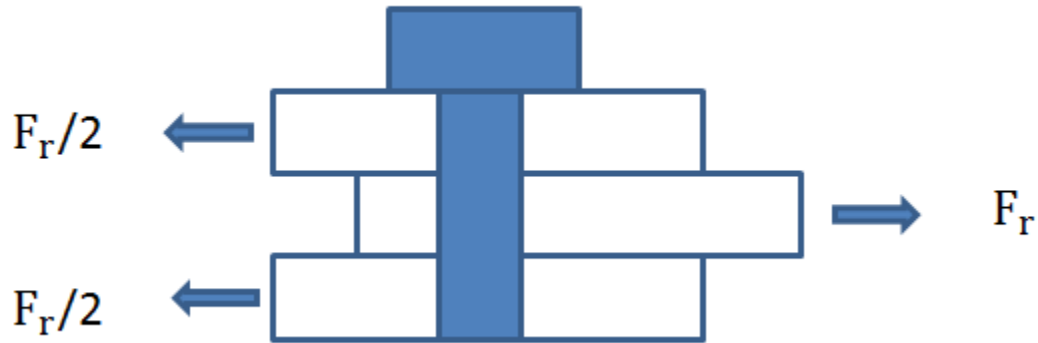


Figure 17 Schematic Diagram explaining the forces on the bolts

Taking into account ultimate tensile strength of 180ksi [16] for black oxide alloy steel bolts, 9/16-12 bolts were selected. These bolts have a tensile stress area of .182 squared inches [19].

2.3.5 Chain Length Calculations

The vertical distance between the roller shaft and the driving shaft is 3.4 inches whereas the horizontal distance between the shafts is 1.5 inches. Thus the distance between the two sprockets was calculated to be 3.762 inches. Number of links required for the chain can be calculated by

$$L = .157 \cdot C + \frac{Z1}{2} + \frac{Z2}{2} \quad (20)[19]$$

where C is centre distance between the two sprockets, Z1 and Z2 are teeth on the two sprockets. From equation 18, number of links was calculated to be at 31.5. The following figure gives a graphic representation useful for calculating chain length.

2.4 Stress Analysis of the Tester.

Part of the tester was simulated in ANSYS Workbench software. This part includes all the load bearing members of the tester. Deformation analysis was carried out on the loading members, roller shafts, guide mechanism, base plate, and I-beams. Normal force was applied to the along the hydraulic cylinder rods. The I-beam supports were fixed.

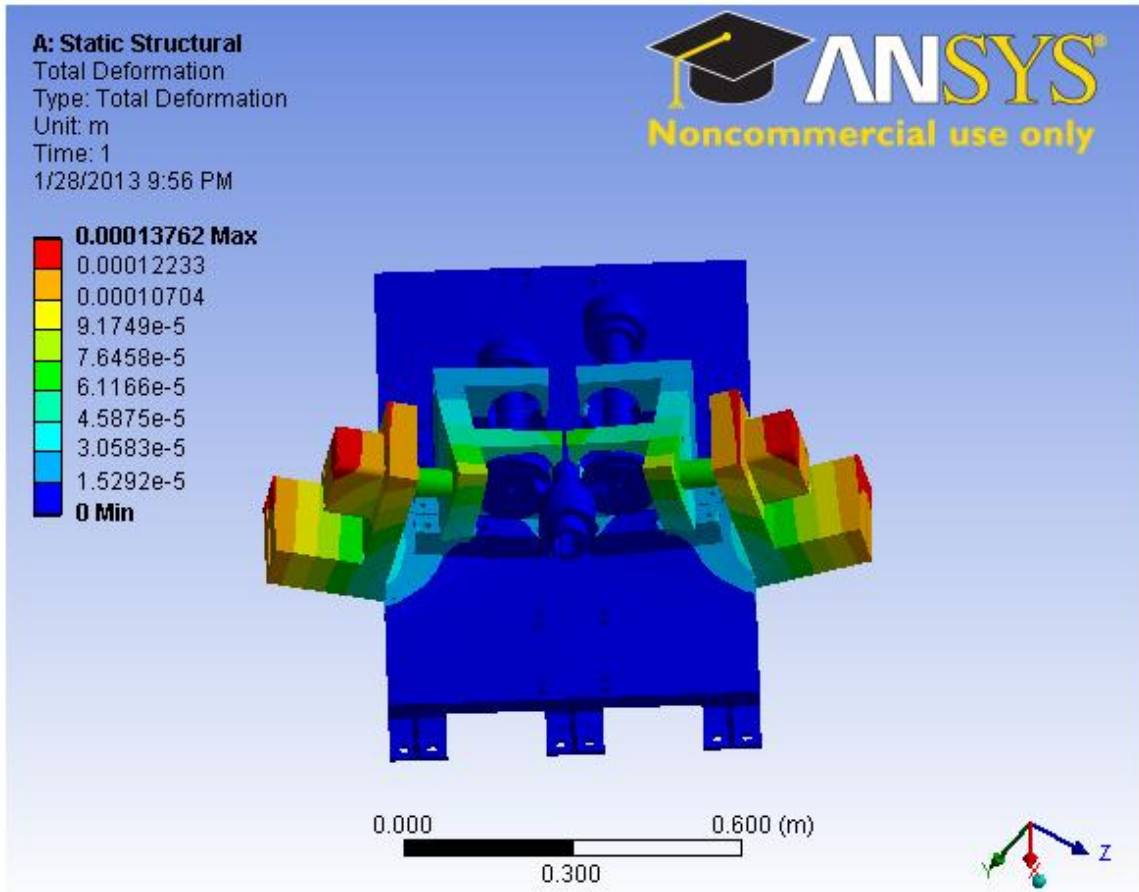


Figure 18 Deformation Analysis of the Tester

Figure 18 gives the results for total deformation in the tester after simulation. The maximum deformation obtained, was in the cylinder mounts, which is 0.13 mm. To reduce the deformation in the cylinder mounts, they were reinforced with gussets and steel tubes as shown in the Figure 19

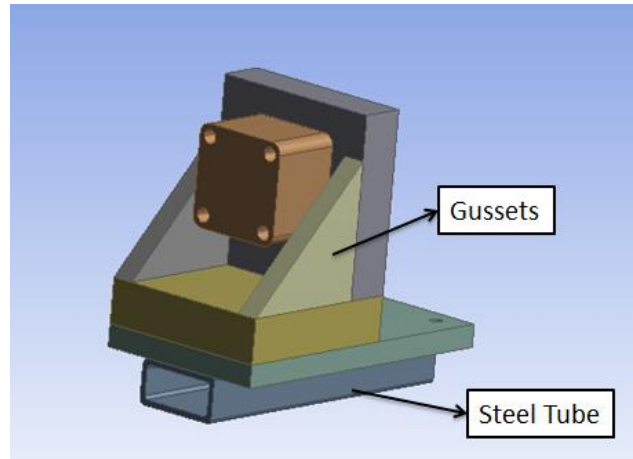


Figure 19 Cylinder Mounts with reinforcement

After reinforcing the cylinder mounts, the total deformation was slightly less than before. The difference in total deformation was negligible after reinforcing the cylinder mounts. But since it was possible to reinforce the cylinder mounts at no extra charge, the cylinder mounts were reinforced.

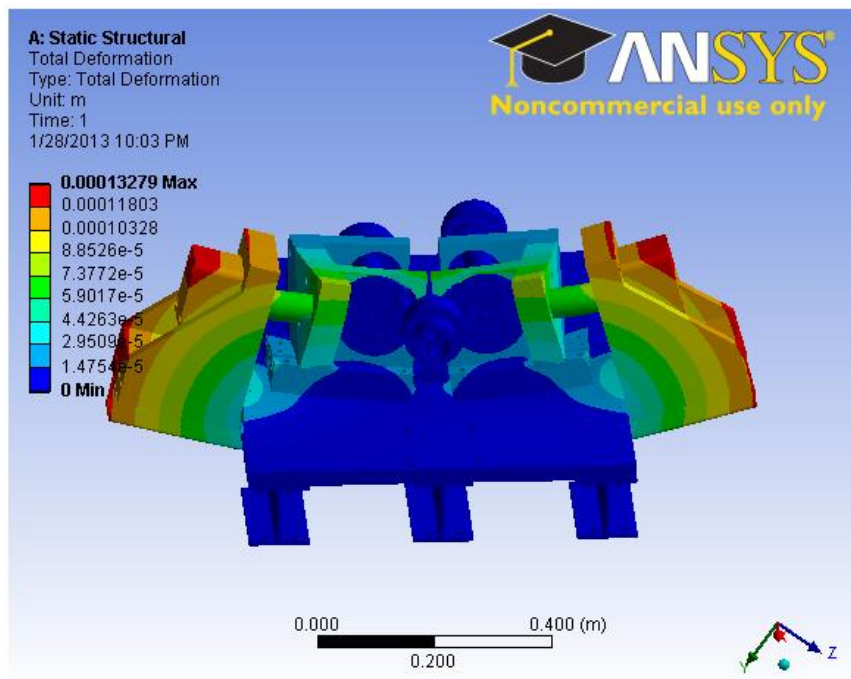


Figure 20 Deformation Analysis of the tester with reinforcement

The maximum stresses were found in the I-Beam. As seen in Figure 21 the maximum stress was 159 MPa. Factor of safety 2 was used in the design, since the material is obtained from a recognized vendor [15]. AISI 8620 steel was used for the structure of the RCF-Tester, since its tensile strength is 384 MPa [19].

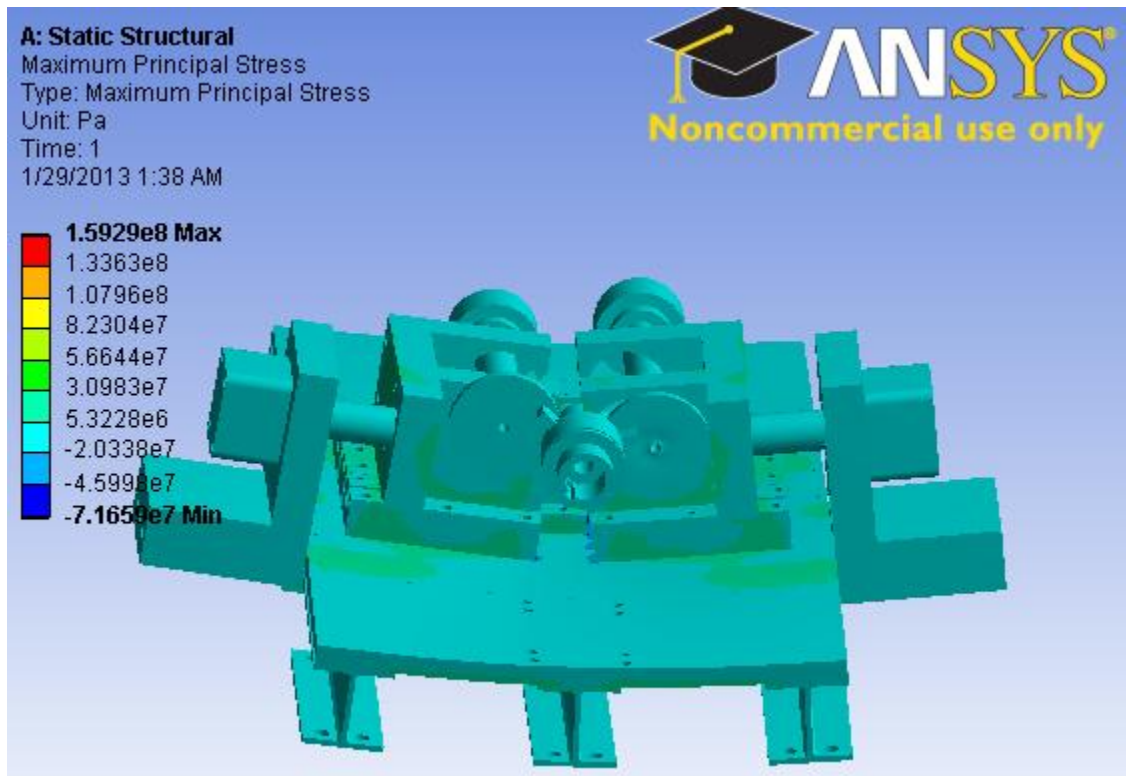


Figure 21 Stress analysis of the tester

2.5 Fatigue Analysis on Rollers and Roller Shafts.

For fatigue analysis obtaining a Stress-Life curve or S-N curve is necessary. A typical S-N curve for steels is showed in the Figure X. Here S is the applied alternating nominal stress and N is the number of cycles to failure. The S-N curves are plotted on log-log scales [1].

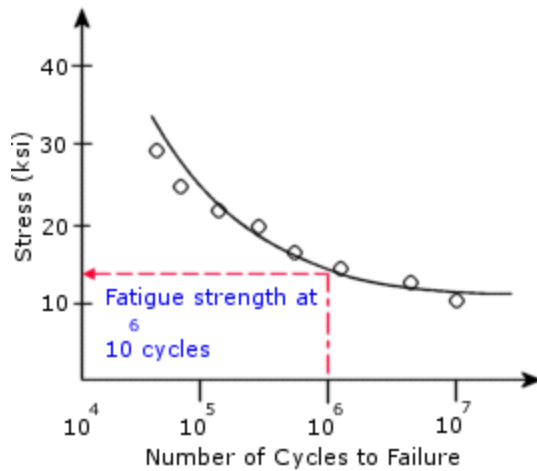


Figure 22 Typical S-N curve [1]

Figure shows a continuous sloping curve with a discontinuity or a knee in the S-N curve. This knee is generally found between 10⁶ and 10⁷ cycles in most steels [1].

Figure shows a more common and reasonable S-N median fatigue life curve. It is based on straight line log-log approximation. This was suggested by Basquin in 1910 [1].

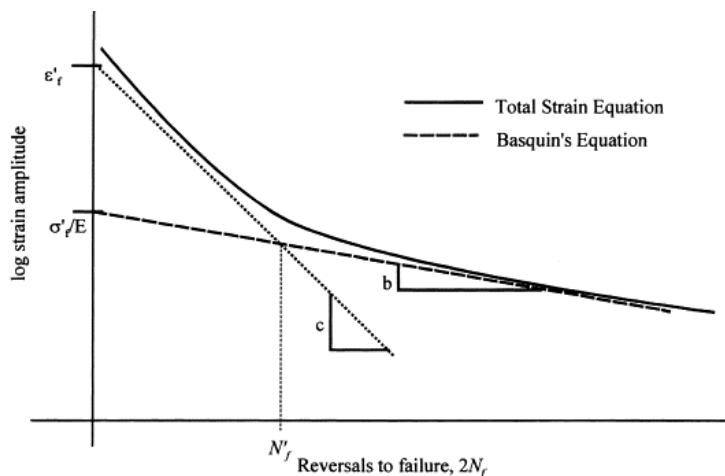


Figure 23 Typical Basquin Curve [1]

In figure region between 10^0 and 10^6 is called as finite life region [1] and the region after the finite life region is called infinite life region [1].

Fatigue analysis was done on roller shafts and the roller assembly using ANSYS Workbench software. The roller shafts and the roller assembly showed life of more than 10 million cycles.

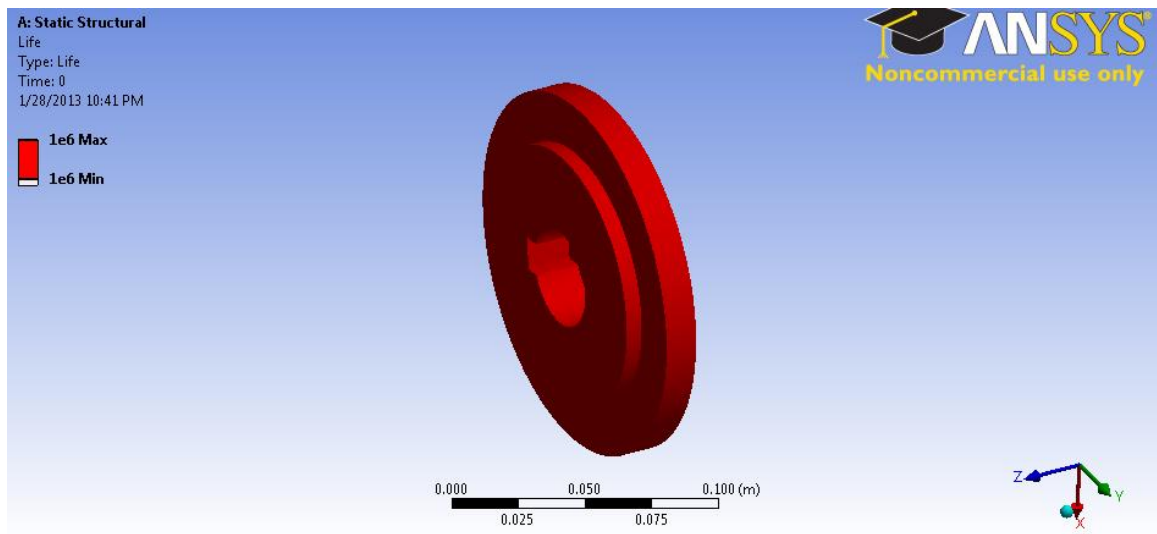


Figure 24 Fatigue Analysis on Rollers

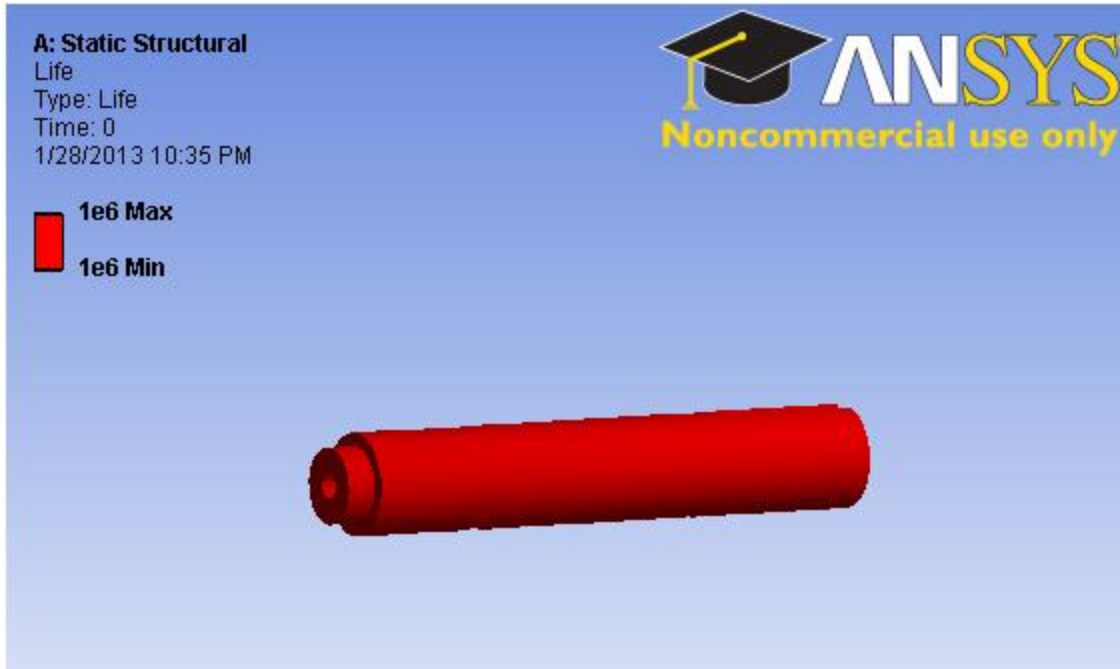


Figure 25 Fatigue Analysis on Roller Shafts

CHAPTER III

ELECTRONIC COMPONENTS OF THE TESTER

This chapter will discuss various electronic components needed for this tester. To detect cracks, an eddy current testing device was selected since it was available from the old tester. This chapter also discusses motor controllers that help keep the speed of the motors consistent with user defined speed. Other components also discussed are data manipulation system and software to help control the tester.

3.1 Eddy current testing device

Eddy current (EC) probes have been in use since a long time now. Eddy current testing began in 1831 as a result of Michael Faraday's discovery of electromagnetic induction [21]. People started using them for searching for gold or for buried treasure or just a sewer line. Using eddy current (EC) principles, common "metal detectors" that sequel at the presence of metallic objects can detect metal at significant depths within the earth or concrete wall without having to Jackhammer an entire concrete wall [21].

EC probes measure a material's response to electromagnetic fields over a specific range, typically a few kHz to several MHz for traditional nondestructive evaluation (NDE) applications. From this response, we can interpret conditions

such as hardness, thickness, presence of corrosion, or defects such as porosity and cracks. The two properties directly interrogated by the EC probe are electrical conductivity (as the term current suggests) and the magnetic permeability. Thus, the method inspects only conductive materials, primarily metals, but also low conductive materials such as graphite-epoxy composites [21].

EC method is a mature, proven NDE technology with a solid theoretical foundation. It is widely represented in industries such as automotive and aircraft manufacturing and it is an integral part of inspection and maintenance in the power generation and aircraft industries. Additionally, EC methods are extensively used in process control [21].

The eddy current method is based on the principle of measuring changes in the impedance of an electromagnetic coil as it is scanned over a surface of conductive material. The following figure shows how eddy current testing works, and helps in detecting cracks [21].

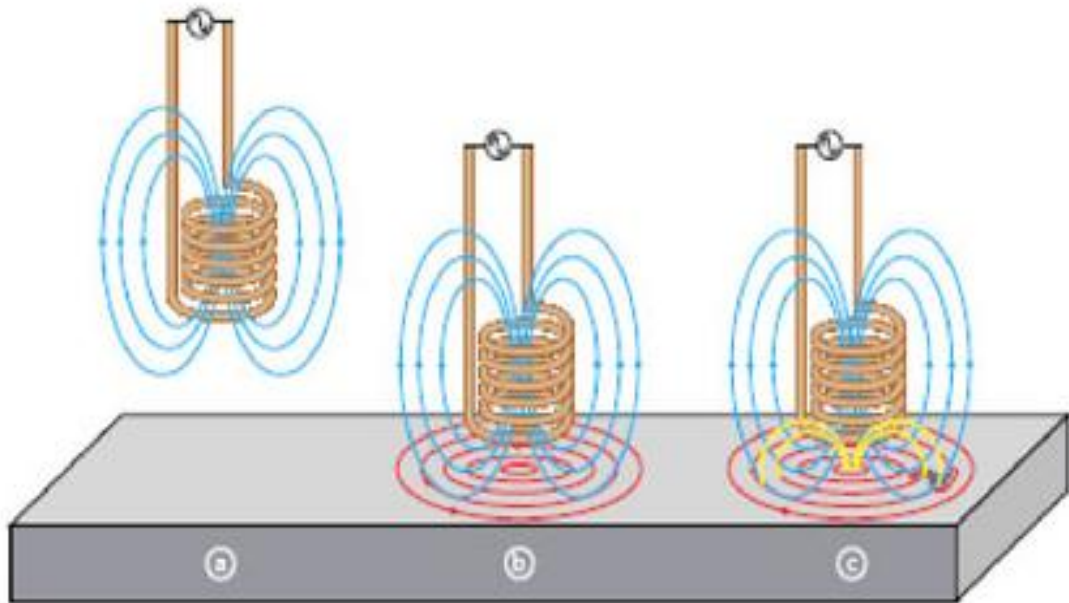


Figure 26 a) The alternating current flowing through coil generating magnetic field, b) Eddy current induced in the material, c) Change in impedance observed due to a flaw [16].

In Figure 26, the magnetic field produced by a AC current are showed by blue lines, the eddy currents formed due to presence of a metal are represented by dotted blue lines, and the yellow lines represent the interruption in eddy currents caused by a flaw or a defect.

The conducting coil used in eddy current testing systems is placed inside a casing called a probe. Probes can come in different types and configurations depending on the application. There are mainly 3 types of probes, absolute, differential, reflection. Absolute probes generally have a single coil and it measures change in impedance. Due to presence of only one coil, these coils are sensitive to lift-off, vibrations, and conductivity [21].

Differential probes have two coils with alternating current passing through them. These probes are sensitive to flaws since they measure the difference in signal between the two coils in the probe. These probes are not sensitive to vibrations, liftoff and temperature. Signal interpretation of this coil may be difficult in case the crack is wider than the spacing between the coils. The spacing between the coils can be as small as 0.1 mm [21].

Reflection probes also have two coils. But in these probes only one coil has current passing through it while the other coil senses the changes in the test material. In reflection probes the coil configurations can be optimized for a specific purpose [21].

The eddy current detection system used in the second generation S-RCF tester is borrowed from the first generation S-RCF tester. It is the Foester Defectomat® EZ 2.828. This device gives the user the flexibility to test with 8 different frequencies. The line speed limitation of this device is 24,000 feet/minute). This means the material below the probe can only have a linear velocity of less than 24,000 feet/minute. A 2.5 inch diameter specimen rotating at 4000 rpm in the S-RCF tester would be travelling at 2100 feet/minute. The probe used in the eddy current inspection system is a differential probe.



Figure 27 Foerster Defectomat EZ 2.828 Eddy Current Detection Device

A lot of factors can affect an eddy current testing device's performance. These factors can be broken down into two categories, electrical properties and surface properties. The material that needs to be tested has to be electrically conductive for eddy currents to be induced in them. The electrical properties of a material can be influenced greatly by alloying, temperature and coatings. Manufacturing processes like hardning, surface finish can influence surface properties [22].

Third category of factors that influence the performance of the device is setup factors. These factors include inspection frequency and lift-off. Figure X below gives us a idea how inspection frequency affects depth of penetration of eddy currents. The sensitivity increases with higher frequency but also reduced the depth of penetration [21].

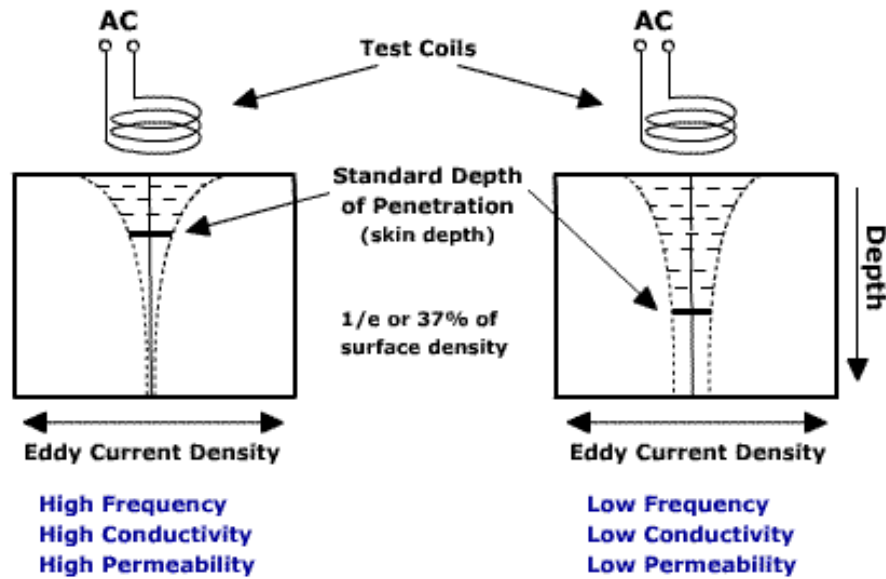


Figure 28 Diagram showing difference in skin depth between different frequencies, conductivities and permeability while using a eddy current device

Penetration of eddy currents is inversely proportional to the frequency. Using a higher frequency will result in lesser skin depth than a low frequency. The density of eddy currents will reduce exponentially with depth into the material.

The depth of penetration can be calculated if some information is available about the material. The characteristics that need to be known about the material are, σ , the material conductivity. μ_m , the magnetic permeability and μ_o , the

permeability of the free space. In case of the second generation RCF tester, the free space will be transmission oil. f_{Hz} is the eddy current inspection frequency.

From these known parameters δ the standard depth of penetration can be calculated in mm [19].

$$\delta = \frac{1}{\sqrt{\sigma \cdot \pi \cdot \mu_0 \cdot \mu_m \cdot f_{Hz}}} \quad (22)[23]$$

A limit frequency is the frequency where the magnetic field penetrating the surface is the strongest and it can be calculated for a curved surface.

$$f_{limit} = \frac{1}{2 \cdot \pi \cdot r_s^2 \cdot \sigma \cdot \mu_0 \cdot \mu_m} \quad (23)[23]$$

The second setup parameter that affects the performance would be lift-off. Lift-off is simply the distance between the probe and the material that needs to be tested. The sensitivity will decrease when the distance between the probe and the piece will increase.

The Defectomat® EZ 2.828 has an oscilloscope on the front panel that has the ability to display the impedance in four different forms (X,Y,Y², XY). The impedance measured by the eddy current device can be broken down into two components. The resistive part of the impedance is the real part and the reactance part of the impedance is the imaginary part. On the oscilloscope the resistive impedance is labeled X since it is usually displayed on abscissa whereas the reactance impedance is labeled Y (ordinate).

3.2 Data manipulation system

This section talks about data collected from the eddy current system. It also talks about storing the data in such a way that it does not use up a lot of space. The data analysis of eddy current signals will also be discussed in this section.

3.2.1 Data storage

In the first generation RCF tester the test parameters that were monitored and recorded were slip ratio, oil temperature, eddy current voltage readings, and applied loading. 8 channels were used; the first four were EC readings. In the second generation RCF tester the oil temperature will not be recorded since the change in the oil temperature is expected to be negligible since the operating conditions are quite similar to the first generation tester and the change in oil temperature in the first tester is negligible. The loading will also be manipulated manually in the second generation RCF tester. If the loading has to be controlled by the computer, servo valves can be used in the future. All these parameters are recorded using a TEAC LX-10 recording unit. The following information is about the channels recorded in the recording unit.

Table 3 Details of conversion factors used for Data Manipulation System

TEAC Channel	Channel Description	Monitoring Unit	Voltage Range	Conversion Factor	Units
1	Y-Component	Defectomat® EX 2.828	0 to 1	1	V
2	X-Component	Defectomat® EX 2.828	0 to 1	1	V
3	V	Defectomat® EX 2.828	0 to 1	1	V
4	Y ²	Defectomat® EX 2.828	0 to 1	1	V
5	Specimen Motor speed	PowerFlex 700S	-10 to 10	416.5	RPM
6	Roller Motor Speed	PowerFlex 70	-10 to 10	416.5	RPM

The conversion factors for the motor speed are the same for the first generation RCF tester and second generation RCF tester since the data manipulation system, the recording units, the motor controllers, the motors, and the eddy current device are the same. The maximum speed of the motors is 4165 rpm and the maximum voltage into the controller is 10 volts. Therefore the conversion factor of the motors was calculated as 416.5 rpm. A signal of 1 volt to the controllers gave an output of 416 rpm, reconfirming the calculations.

The next step would be to decide how to record the information. The RCF tester would be testing specimens at about 3000 loading cycles per minute. That would take AISI 8620 specimens approximately 33 hours to fail considering average cycles for failure to be 6 million cycles at 2.1 GPa Hertzian stress. The amount of cycles will go down drastically as the Hertzian stress is increased.

Considering the significant amount of time, continuous data storage is not a reasonable method. Another factor to be considered would be that no two specimens will fail at around the same load cycles. Taking all these factors into account, the data recording at user specified intervals was chosen as the best method. The TEAC LX-10 recording unit comes with a program called LX-NAVI. This program was used to record data intervals. The data at intervals are recorded into a header and data files format.

After opening LX-Navi and before setting up different parameters to be setup, new file must be opened for every recording session. This is done by either pressing ctrl+n or by clicking 'new' in file drop tab. The file is saved as s (for specimen), followed by specimen number and then followed by an F (for file). The recording option should be selected as the PC since the storage device is the PC.

The number of zeroes after the file name is set to five. Setting the zeroes to five will mean that 99,999 files can be created in that testing session and the file name will start form 00001. If anything else is used, for example number of zeroes is set to 6, first file name will be 000001. If the number of zeroes is changed, the Matlab® files need to be modified so that Matlab® will be able to open those files. Now the system parameters can be set up. For setting up system parameters click 'system' under the Setup tab. For the second generation S-RCF tester, only the system tab and slot (PA-8) tabs are used.

The number of points that will be recorded every second is determined by sampling rate. In LX-Navi the sampling rate can be set under the system tab. The value of sampling rate depends on the speed of the specimen and the area that is being recorded. This value can be determined by the following equation. Here w_d is the width of the specimen and r_s is the radius of the specimen. The sampling rate S can be calculated by the following equation.

$$S = \frac{2 \cdot \pi \cdot r_s}{w_d} \quad (24)$$

The minimum recording frequency also needs to be determined. The recording frequency can be calculated with the help of w_s (rotational speed of the specimen)

$$F_m = S \cdot w_s \cdot 2 \quad (25)[23]$$

The maximum speed of the S-RCF tester is limited to 4000 rpm due to the sprocket chain mechanism used. The scanning area of the eddy current testing probe that will be used is 5 mm. But since the area that is being scanned is curved, the scanning width should be 1mm. Considering this, the frequency at which the data is collected is calculated to be 14 kHz. The closest frequency in LX-Navi is 24 kHz.

The clock can be synchronized with the clock of the PC. The next value that needs to be set up is the number of channels to record. Six channels should be selected under slot 1, since these are the number of channels needed. Slot1 (PA-8) is the system window in the second tab. Each channel can be calibrated

manually or automatically by slot 1 (PA-8). In auto mode LX-Navi will measure the current voltage and calibrate itself. In this mode the signal is expected to rise during a defect. Hence auto mode is not advisable. The voltage values that can be set in LX-Navi are .01, .0316, 1, 3.16 or 10 volts. The channels 1 to 4 meant for eddy current detection device are set at 3.16 volts. Channels 5 and 6 are set at 10 volts.

The information that is being recorded will be taken by the user at specified intervals. Then parameter that needs to be setup for the LX-Navi is the trigger for recording unit. The trigger window is accessed by clicking the trigger button in the main LX-Navi. The trigger window will help in changing a lot of parameters like recording time, interval time, and start time. This can be done by selecting interval check box. The start time is the time when the first data will be recorded to the first file. After setting start time, RecTime and Interval Time need to be set. The RecTime is the time for which the data will be recorded. Interval Time is the time between two recordings. Each of these recorded files represents the second generation S-RCF tester over a period of time. Number of load cycles (LPCF) can be calculated by known parameters like specimen speed ω_s , Recording Time R_L , and Interval Time I_L in seconds. The factor 2 represents the number of contact points.

$$LPCF = \frac{\omega_s \cdot 2 \cdot (R_L + I_L)}{60} \quad (26)$$

As the record time and the interval time increase, number of load cycles that go unrecorded will decrease. The number of specimen rotations Rev_f in each file

can be calculated by removing the factor 2 and interval time from the above equation.

$$\text{Rev}_f = \frac{\omega_s \cdot R_L}{60} \quad (27)$$

3.2.2 Data Analysis

The data that has been recorded by LX-Navi can be viewed by another program called LX-View. Number of files can be exported into LX-View using the batch convert option. LX-View can also export information into several other file formats. In case the batch convert option does not work, run Teac2Matlab file. Teac2Matlab is located in Appendix B. Teac2Matlab file will convert all the .hdr files recorded by teac and save as a bitmap image.

The inputs required to run the Matlab® files are located in the file TestingParametersValues. The following table provides a detailed view over the values required.

Table 4 Inputs required for Matlab® Files

Variable Name	Description	Units
Intervaltimemin	Interval time to check if crack has occurred	Min
specs_to_read	Time to read each file	S
specimennumber	Specimen Test Number	
Reclenght	Time each file is recorded	S
Recinterval	Time between each file recording	S
Specms	Specimen motor speed	RPM
Slipratio	Slip ratio between surfaces	
IVc1	Initial maximum value for channel 1	
IVc2	Initial maximum value for channel 2	
IVc3	Initial maximum value for channel 3	
IVc4	Initial maximum value for channel 4	
IVc5	Initial value for channel 5	
IVc6	Initial value for channel 6	
deltaC1	Maximum Allowable Change for channel 1	V
deltaC2	Maximum Allowable Change for channel 2	V
deltaC3	Maximum Allowable Change for channel 3	V
deltaC4	Maximum Allowable Change for channel 4	V
deltaC5	Maximum Allowable Change for channel 5	%
deltaC6	Maximum Allowable Change for channel 6	%

Processing this kind of large information in an outdated student version of Matlab® can take too much time. To process this information in short period of time, the data saved is analyzed in three stages, failure detection stage, screening stage and the analysis stage. A separate file is written for each stage. The file for failure detection stage is RealTimeDataAnalysis.

A flowchart is shown below which describes the failure detection stage.

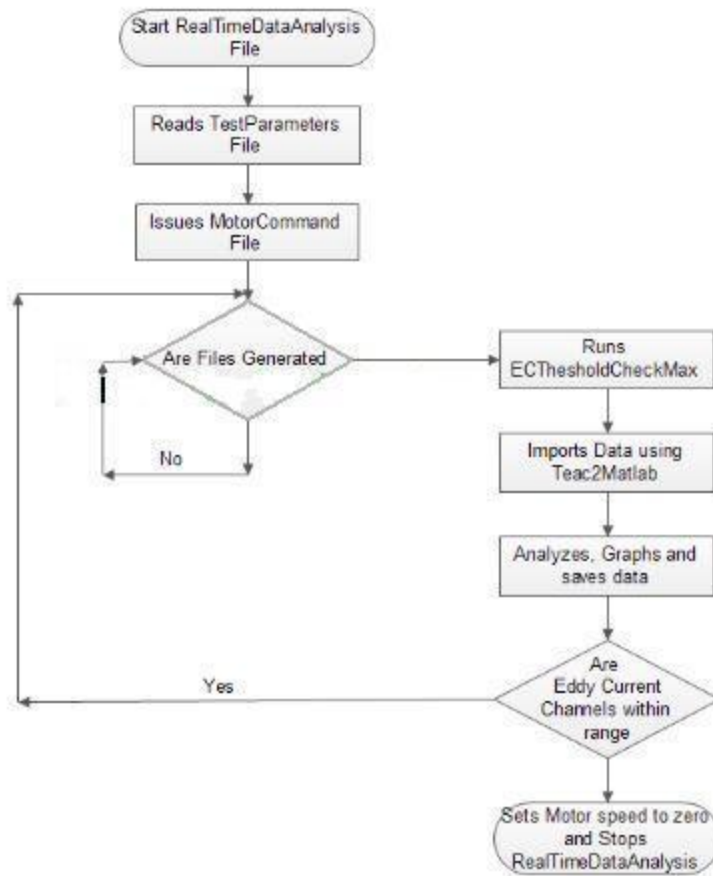


Figure 29 Flowchart of failure detection system

The first step to begin the testing and starting the machine is to run RealTimeDataAnalysis. When this file is started the motor controllers will receive voltage sent by motorcommand file. The motorcommand file uses a NI PCI-6251 card connected to a NI BNC-2110 terminal block. Once the motors start running the program waits until the data file corresponding to intervalmin variable is generated by the TEAC recording unit.

At this point the RealTimeDataAnalysis calls upon ECThresholdCheckmax file. The main function of this file is to bring in the data using Teac2Matlab file.

EThresholdCheckmax also filters down values in each file to its absolute maximum and absolute minimum values. These values are converted into meaningful values using the conversion table. These maximum and minimum values are user specified and are plotted on two figures. First figure contains plots of channels 1 to 4 and figure 2 contains plots of channels 5 and 6. These plots are saved in the same folder as the data being recorded as bitmap.

The last function of EThresholdCheckmax is to monitor the eddy current channel's readings. If the maximum voltage is outside the range of the user specified range then the motorcommand file will automatically stop the motors otherwise the program resets itself and waits for the next time interval to check again.

CHAPTER IV

TESTING PROCEDURE

In this chapter the test setup and disassembly procedures used when performing fatigue testing with the RCF tester will be discussed. This chapter also discusses various steps that need to be taken before starting a test like measuring specifications of the specimen. The testing conditions and failure criteria will also be discussed in this chapter along with the eddy current calibration device, which helps to set eddy current parameters.

4.1 Test setup procedure

After setting up the machine the specimen and the rollers can be ordered. The drawings of both will be found in Appendix E. Along with the dimensions, several other parameters can be specified. Parameters like surface roughness, microstructure, hardness and composition can be specified. The roughness of the specimen will depend on the superfinishing process. Hardness and microstructure depends on the heat treatment of the specimen.

Once the specimen has arrived, verifying its properties would be the next step. Physical characteristics like its dimensions can be measured using a caliper. For detecting cracks, eddy current tests can be carried out. The surface

roughness of the specimen can also be measured using the Surfcom 480A profilometer. The profilometer comes with a stylus that can be moved across the surface of the specimen to measure the change in height. This device gives the user a printout of several roughness parameters.

Once the quality of the specimen is verified, the RCF tester can be setup. First, move the linear guides outwards to its maximum limit. This would allow setting up the specimen without any problem. After moving the linear guides, the rollers can be inserted on top of the roller brackets. The roller brackets are meant to stay on the shafts permanently and should only be removed in case of damage. After setting up the rollers, the specimen can be inserted in the 3 jaw mandrel chuck. The live center should be positioned at this point to support the specimen. Now the oil tank can be filled up with transmission fluid. Once the oil tank is filled, the cover of the oil tank can be attached to the walls.

The eddy current probe is then inserted in the machine from the top. The gap between the specimen and the eddy current probe can be measured using a feeler gauge. But this distance cannot be measured after the cover is already in place. So this distance should be calibrated on the probe holder beforehand. The RCF is now fully assembled.

The eddy current device needs to be powered on now. There are several input parameters that are required to be calibrated and adjusted to obtain some meaningful results including inspection frequency, sensitivity, line speed, high

pass filter value and low pass filter value. These values can be changed by using setup buttons on the front panel of the eddy current device.

The depth of penetration into a material depends on the inspection frequency. The frequency is inversely proportional to depth of penetration. A low frequency would result in high depth of penetration but low surface eddy current density. A high frequency would result in low depth of penetration but high surface eddy current density. A high frequency is used when the concentration is more on surface failure. A low frequency is used when the concentration is on subcase failure.

The line speed function of the eddy current device lets the system know how fast the specimen is moving under it. Essentially, it is the surface velocity of the specimen. The line speed setting will allow the high pass and the low pass filters to be set. High pass filters filter out unnecessary high frequencies received by the probe. Low pass filters filter out low frequencies. High pass filters and low pass filters are useful to reduce the noise received due to vibrations from the machine. The eddy current system, Defectomat EZ 2.828, has appropriate settings for the filters based on line speed of the specimen.

The sensitivity of the system can be adjusted. Its maximum value is set at 62.5 dB. The sensitivity will allow the output of a flaw to be greater or lower. It should be calibrated for different materials and different flaw sizes. After setting up the eddy current system, the TEAC LX-10 recording unit is powered on. Now

the computer can be turned on. The computer will not recognize the LX-10 if it is not on when the computer boots up.

After the computer is turned on, the recording program needs to be set up. LX-Navi will be used as the recording program for the S-RCF tester. Details of this program can be found in Chapter II. Before starting the LX-Navi, one has to remember to setup the file settings. After opening LX-Navi, click new file under file tab. The file name, number of zeroes in the file name and the PC recording option can be set in this window. The next step is to set system parameters. This can be done by clicking on the system button in the main window or by clicking system in the setup drop menu. When the system window is opened, under the system tab, the clock for LX-Navi can be synchronized with the PC, the sampling rate can be set and number of channels to record can be set as well. The calibration value can be set for each channel under slot1 (PA-8). Now set up the trigger for LX-Navi. The properties for this can be changed using the trigger window by clicking trigger button on the setup drop menu. Check the box by the interval option in the trigger window. The values that need to be set for the trigger are record time, record interval time, repeat count and start time.

After recording program is set up, seven Matlab® files are dragged into the directory where the data files will be created. These files include T2Mv2screening, T2Mv2Analysis, TestParametersValues, Teach2Matlab, RealTimeDataAnalysis, MotorCommand and ECThresholdCheckmax. Only the last five files mentioned are used during testing. Once the test is completed and further analysis is performed the first two files are listed.

Once all the files are in place, the motors can be turned on. Turn on the power on the motors and controllers by flipping 13-15-17 and 37-39-41 breaker groups in the breaker box.

Matlab® would be the last program to be started and setup. Once the Matlab® is opened, its working directory need to be setup. The working directory would be where all the files are located. Now, open the TestParametersValues file and enter the values for the test to be performed. Some of the parameters whose values that need to be entered here are the speed of the motor, interval time to check if crack has occurred, specimen test number, etc. Save the file after entering the parameters.

Determining initial values would require the machine to be started and data to be recorded briefly. First step for determining initial values, go to the prompt window for Matlab® and type TestParametersValues and press enter. This will place the test values into memory by running TestParameteresValues. Now the motors can be started. First turn on the motor switch. Now run the motorcommand in the prompt window. This will send voltages to the motor controllers. Once the motors are running and have reaches a desired value, the initial values can be read.

The initial values can be either observed visually, by reading the values using digital readout available in the LX-Navi program. Or the initial values can also be obtained by recording files to analyze.

The digital readouts can be activated by activating the digit button in the main LX-Navi window or by clicking digit under the view drop box menu. One can also bring up multiple digital readouts by clicking digit button in the digital readout window. Each of these readout windows are set to a specific channel the readout will show the current value only after the recstandby button is clicked on.

The initial values can also be recorded by recording files to analyze. Even though this method is more time consuming, it is certainly more accurate way of getting initial values. These files are created by clicking recstandby button in LX-Navi button in the main window. This button will remain depressed indicating that the program is ready to record values. Clicking the play button will record a file for the interval the user specified in the trigger window. To achieve an accurate representation of the values, several files should be recorded and analyzed. The only drawback of this method would be that new files need to be setup. In case a new file is not setup, the file numbering will continue from the last file the user created manually.

After reading the initial values, the motor controller switch need to be turned off. Now enter the values in TestParametersValues file and save the file. The next step would be to determine maximum allowable change for each channel. This would determine when the machine will stop. These values are entered as an increment of voltage change from the initial value. The voltage change corresponds to a certain size defect or anomaly on the surface of the specimen. Calibration of material and different size specimens is necessary to enter allowable change in voltage. The maximum allowable changes for all these

channels can be entered in TestParametersValues file as a percentage of initial value. After entering the allowable change value the file can be saved and closed.

The S-RCF tester can be used for testing the specimen now. Open the trigger window in LX-Navi and set a appropriate time. Now press the recstandby button. For the trigger option to work, this button needs to be depressed. Run RealTimeDataAnalysis by opening the prompt window and entering the file name and pressing enter. This will bring the initial values into computers memory and will send voltage to the motor controllers. A window prompt will appear telling the user to start the recording system. Now turn on the motor switch. Click OK button once the start time has passed.

The machine should be observed initially to make sure that the MATLAB® graphs are providing a reasonable data. The machine will stop running once the eddy current device receives change in voltage more than allowable change defined by the user.

First step after conducting an experiment would be to turn off the motors, turn off the hydraulics, bring back the cylinders and close down any programs that are running. To inspect the specimen, remove the cover of the oil tank. Slide back the loading mechanism to its extreme outward position. Unlock the specimen from the chuck and remove it for further inspection. Incase just visual inspection is required, and a rerun is needed just put the specimen back in the tester and repeat the procedure all over again.

4.2 Testing Conditions and Failure Criteria

The material that was tested is AISI 8620. AISI 8620 was tested in first generation S-RCF tester. AISI 8620 is a common gear material and some data is available on that material [4]. A total of 5 specimens were ordered from Northern Valley Machine Inc in Grand Forks, North Dakota. The specifications of the specimen can be found in Appendix E

The failure criteria can be set by the user. In some cases a detection of a small crack can be set as a failure or in some cases a large crack can be set as failure criteria. In some tests considerable pitting might be considered as failure. To understand the output of the eddy current testing device a specimen with a crack is required to be tested. From this output the maximum allowable change in the voltage can be determined and set in Matlab® program. The flawed specimens can be spun in eddy current calibration device (ECCD). The maximum speed in ECCD is 1755 RPM. The ECCD can be used to test specimens with flaws using older probes from first generation S-RCF tester.

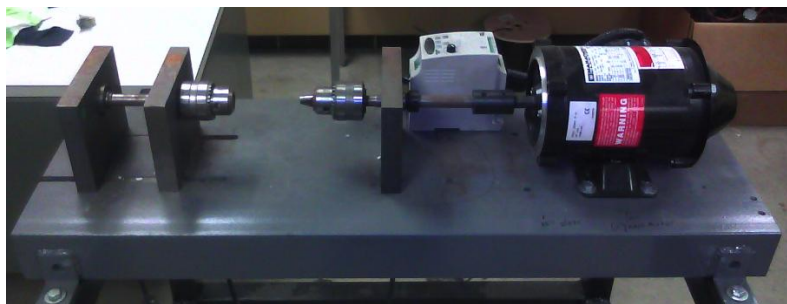


Figure 30 Photo showing ECCD system

In the first generation RCF tester, no failure criterion was set for the sample specimen. The machine was run until the eddy current value reached a value believed to be failure. For all the other specimens a voltage difference of .15 on any eddy current channels was set as failure criteria. A similar criterion has been set for the second generation S-RCF tester. After the voltage increase of 0.15 occurred the machine will stop itself.

CHAPTER V

RESULTS AND DISCUSSION

In this section the preliminary test results are presented along with discussion of these results. The results include fatigue results. This section will also focus on improvements on the tester. All the rollers were made from AISI 8620 and were heat treated. The heat treatment specifications are available in Appendix D. All the specimens were also made from AISI 8620

5.1 RCF Test Bench

To simulate real loading conditions of a gear set is not just almost impossible but also expensive and time-consuming. Taking this into consideration, the tests under simulated conditions are carried out as close as possible. The second generation RCF tester is able to simulate contact fatigue. The two important capabilities of a RCF tester are

- 1) Be able to establish contact and rolling between the specimen and rollers
- 2) Tests performed in lubrication regime 3. Under this regime the surface wear is at minimum.

5.2 AISI 8620 specimen

5 specimens were orders from Northern Valley Machine in Grand Forks. The specimens were made from AISI 8620. The specimens were heat treated to 60 HRC and had surface roughness of 16 to 20 μ inch.

5.3 Test Procedure and Parameters

The test conditions are summarized in table 5 and the parameters for setting up eddy current device are summarized in table 6. After the hydraulic pressure was set at the defined level, the tester was run at 1500 rpm. First few readings were used to determine the level of noise recorded by eddy current testing device. The noise is usually observed due to surface roughness, roundness of the specimen. The noise was observed at about .5 to .15 V. the threshold was set at .15V above the background noise.

Table 5 Test Conditions

Test Rig	S-RCF Test Bench
Contact Pressure	2.45 GPa
Number of load cycles per revolution	2
Speed	1500 RPM
Number of load cycles per hour	180,000 load cycles/hr
Sliding ratio	0%
Oil	Dextron III
Temperature	Room Temperature

Table 6 Setting of eddy current instrument

Eddy Current Instrument	Foester Defectomat EZ 2.828
Coil Excitation Frequency	1000 kHz
Evaluation mode	Phase independent vector
Sensitivity	25 dB
Threshold	.15 V
Data Acquisition system	Teac
Recording speed of the test rig	1500 RPM
Line Speed	2.99 m/s
High pass filter	7
Low pass filter	5

5.4 Results

The first specimen was tested to observe the machine. This specimen ran for about 2 million cycles without any damage. During this trial no problem was observed. The hydraulic system ran without any problems. Both the hydraulic cylinders would deploy at different times, this problem was fixed by adjusting the rods screwed onto the hydraulic cylinders. No drop in the pressure was observed. The eddy current system was working fine. The second specimen was tested under similar conditions. This specimen lasted for about 4 million cycles. Pitting was observed on the specimen as seen in the following figure. Except for the computer hanging once, no other problems were faced in the programming and the data manipulation systems.

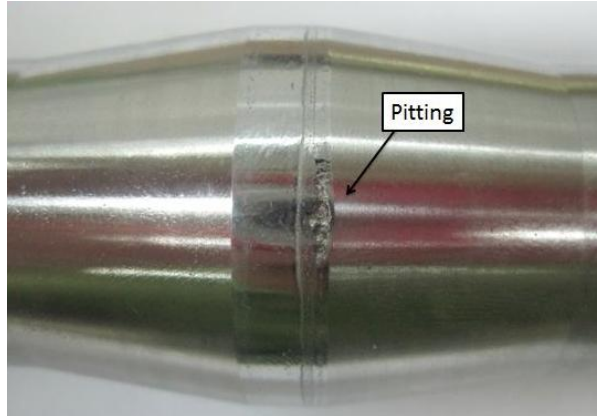


Figure 31 Pitting observed on Specimen 2

For a hertzian stress of 2.5 GPa, 4 million cycles was expected. Specimen 3 was also tested under similar conditions. But after 2 million cycles the experiment was stopped because the bolt used to keep the left roller in place had broken off, with half of it still stuck in the shaft.

Chapter VI

CONCLUSIONS AND RECOMMENDATIONS

The goal of this project was design, fabrication, and verification of second generation RCF tester. When the load cycles of AISI 8620 were obtained and compared to its load cycles available from other testers, it was concluded that the S-RCF tester's performance was good.

The hydraulic system of the tester performed really well. The chains were little loose, idler sprockets were tried out. Since the idler sprockets failed to tighten up the chain, they were replaced by Teflon bars. First the oil tank was sealed using gaskets. Three different type of gaskets were tried but all of them failed. The oil tank was later sealed using JB weld. The oil tank did not leak. The whole machine including the motors was quite stable and did not vibrate much. The eddy current device and the software performed very well.

After working on the present tester, a recommendation was made. Servo valves can be used in the future on this tester for fine tuning the deployment of the two cylinders simultaneously.

APPENDICES

APPENDIX A

Matlab® files

Teac2Matlab file

```
function
[x,dt,date,time]=Teac2Matlab(mins_offset,secs_offset,secs_to_read,fname,EndFile);
clc
close all
%cd C:\matlab\GX-1\ %DADISP_GX.M
%Copy of the file TAFFmat_gx.m sent by Steve Astulfi
%Additions by C.S. Hayek, JHU/APL, 10/16/02
%This is the working copy to install improvements

%Input Variables:
%Scalars-
% mins_offset - the number of minutes to skip before starting to read data
% secs_offset - the number of seconds to skip before starting to read the
% data
% Output Variables:
% Matrices-
% dt-time sequence of data for all channels, in original engineering units
% Vectors-
%x-time, in seconds
% [fname,pname]=uigetfile('C:\Data\Spring2008\ESC\TeacMatlab\*.hdr')
%addpath(pname);
%fid=fopen(fname,'r');
%fid=fopen(fname,'r');
fileexist=0;
while fileExist==0
    try
        fileExist=1;
        fid=fopen(fname,'r');
        fseek(fid,0,1);
    catch
        fileExist=0;
        if EndFile>=15000;
```



```

        fileExist=1;
    end
end
end
%fseek(fid,0,1);
fsize=ftell(fid);
fseek(fid,0,-1);
%fprintf('Reading header info...\n')
[F,count]=fread(fid,[1,fsize],'char');
s=setstr(F);
fclose(fid);
p=findstr(s,'DATASET');
for q=p:fsize
    if F(q)~=13
        else
            break
        end
end
dataset=s(p+8:q-1);
p=findstr(s,'VERSION');
for q=p:fsize
    if F(q)~=13
        else
            break
        end
end
version=s(p+8:q-1);
p=findstr(s,'series');
for q=p:fsize
    if F(q)~=13
        else
            break
        end
end
series=S(p+7:q-1);
p=findstr(s,'DATE');
for q=p:fsize
    if F(q)~=13
        else
            break
        end
end

```

```

    end
end
date=s(p+5:q-1);

p=findstr(s,'TIME');
for q=p:fsize
    if F(q)~=13
        else
            break
        end
end
time=s(p+5:q-1);

p=findstr(s,'RATE');
for q=p:fsize
    if F(q)~=13
        else
            break
        end
end
rate = s(p+5:q-1);

p = findstr(s,'VERT_UNITS');
for q=p:fsize
    if F(q)~=13
        else
            break
        end
end
vert_units = s(p+11:q-1);

p = findstr(s,'HORZ_UNITS');
for q=p:fsize
    if F(q)~=13
        else
            break
        end
end
horz_units=s(p+11:q-1);

```

```
p=findstr(s,'NUM_SERIES');
for q=p:fsize
    if F(q)~=13
        else
            break
        end
    end
end
num_series=s(p+11:q-1);
```

```
p=findstr(s,'STORAGE_MOD');
for q=p:fsize
    if F(q)~=13
        else
            break
        end
    end
end
storage_mod=s(p+12:q-1);
```

```
p=findstr(s,'NUM_SAMPS');
for q=p:fsize
    if F(q)~=13
        else
            break
        end
    end
end
num_samps=s(p+10:q-1);
```

```
p=findstr(s,'FILE_TYPE');
for q=p:fsize
    if F(q)~=13
        else
            break
        end
    end
end
file_type=s(p+10:q-1);
```

```
p=findstr(s,'SLOPE');
for q=p:fsize
    if F(q)~=13
        else
```

```

        break
    end
end
y_slope=s(p+6:q-1)

p=findstr(s,'X_OFFSET');
for q=p:fsize
    if F(q)~=13
        else
            break
        end
    end
end
x_offset=s(p+9:q-1);

p=findstr(s,'Y_OFFSET');
for q=p:fsize
    if F(q)~=13
        else
            break
        end
    end
end
y_offset=s(p+9:q-1);

% disassemble series
nch=str2num(num_series);
p=1;
q=findstr(series,',');
for l=1:nch-1
    label(l)=cellstr(series(p:q(l)-1));
    p=q(l)+1;
end
sz=size(series);
label(nch)=cellstr(series(p:sz(2)));

% disassemble series
p=1;
q=findstr(vert_unitd,',');
for l=1:nch-1
    y_unit(l)=cellstr(vert_units(p:sz(2)));
    p=q(l)+1;
end

```

```

end
sz=size(series);
y_unit(l)=cellstr(vert_units(p:q(l)-1));
% sampling frequency
sampF=str2num(rate);
% horizontal unit
x_unit = horz_units;
% slope
p = 1;
q = findstr(y_slope,',');
for l=1:nch-1;
    slope(l)=str2num(y_slope(p:q(l)-1));
    p=q(l)+1;
end
sz=size(y_slope);
slope(nch)=str2num(y_slope(p:q(l)-1));
%offset
p=1;
q=findstr(y_offset,',');
for l=1:nch-1
    offset(l)=str2num(y_offset(p:q(l)-1));
    p=q(l)+1;
end
sz=size(y_offset);
offset(nch)=str2num(y_offset(p:sz(2)));
%read data file
p=size(fname);
fname=fname(1:p(2)-4);

fname=strcat(fname, '.dat');
fid=fopen(fname,'r');

% Compute the number of bytes to skip into the data, based on user's input
% (S. Haayek, 10/16/02)
secs_into_data=(mins_offset*60)+secs_offset;
nbyteskip=secs_into_data*sampF*nch*2; % the 2 is to allow for 2 byte data
words
statusR=fseek(fid,nbyteskip,'bof');
if statusR==-1
    message=ferror(fid)

```

```

    return
end;
% compute the number of EKEMENTS (not bytes) to read, based on user's input
% (S. Hayek, 10/16/02)
nelread=secs_to_read*sampF;

%fprintf('Reeading Data ...\n')

%[dt,count]=fread(fid,[nch,inf],int16); % Astulfi's original
[dt,count]=fread(fid,[nch,nelread], 'int16');
fclose(fid);

% convert data
for l = 1 : nch
    dt(l,:)=(dt(l,:)*slope(l)+offset(l));
end

% calculate data number
ndata=count/nch;

% create X
%x=linspace(0,ndata/sampF,ndata); % Astulfi's original
%x=linspace(0,ndata*samF,ndata);
x=linspace(secs_into_data,secs_into_data+(ndata/sampF),ndata);

```

RealTimeDataAnalysis File

```
clear all
close all
clc
%-----
%user inputs (create a load file for these values)
TestParametersValues
speedup=30;$(s)FOR TESTING ONLY SET TO 1 OTHERWISE
intervaltime=intervaltimemin/speedup;
%-----

StartFile=1;%First File to REad on the first Loop
%need to substract off the pause time for the graphs
%-----
%Send Start Command
motorcommand %calls up .m file to send motor voltages
%voltages are maintained at the last value?
%-----
%Pause to Start TEAC recording
fprintf('Please start TEAC recording.\n\n')
prompt={'Press any button to begin Analyzing Data'};
title='Start Test';
lineNo=1;
inputparam=inputdlg(prompt,title,lineNo);
%-----
starttime=clock;%Start time of the program
%-----
%Data analysis to determine if machine should stop
MyStop=0, % Machine stop command
intervalcount=1; %counts the number of times the data is checked
EndFile=StartFile-1+intervaltime*speedup*60/(reclenght+recinterval);
%End File for first loop
while MyStop==0;
% elapsedtime=etime(clock,starttime;) % elapsed time in seconds
% if elapsedtime>=intervaltime*60*intervalcount;
% command to start at interval mark
% while elapsd time>=intervaltime*60*intervalcount;
ECThresholdCheckmax %file to load and check max value
StartFile=EndFile; % New First File is the last loops EndFile
```

```
EndFile=EndFile+inervaltime*speedup*60/(reclenght+recinterval);
% New Last File HEader to Read
intervalcount=intervalcount+1; %Looping count number
% end
% end
end
%-----
%issue stop command
specms=0;
rollms=0;
motorcommand %calls up .m file to send motor voltages
```


Motorcommand file

%Machine Values

rspec=.0381/2; %(m)Radius of specimen

rroll=spec*3; %(m)Radius of Roller

RPMtoVolt=416.5; % converts RPM to Voltage

specsv=specms/60*(2*pi*rpec); %(m/s) specimen surface velocity

rollsv=specsv*slipratio; %(m/s)roller surface velocity

rollms=rollsv/(2*pi*rroll)*60; %(RPM) Roller motor speed

specmv=specms/RPMtoVolt; %(V) specimne motor voltage

rollmv=rollms/RPMtoVolt;*(V) Roller Motor Voltage

ao=analogoutput('nidaq','Dev2'); % specifies the device type and ID number

channels=addchannel(ao,[0,1]); % specifies channels to use for ao

set(ao,'SampleRate',8000); % sets the sample rate property

t=linespace(0,1,16000); %linear space from a tp b with n points

y=specmv*ones(1,size(t,2)); %voltage data for specimen

y1=rollmv*ones(1,size(t,2)); % voltage data for motors

putdata(ao,[y'y1']); %queue data to be sent on each channel

set(ao,'TriggerType','Immediate'); %when to start the data floe

start(ao);

wait(a0,5);

clear y y1 ao channels t

EThresholdCheckmax File

```
clc
%
%Inputs
%-----
tc=0;%min Time correction value if time went
%unrecorded and for a second group of files
%-----
%this section reads the header files and brings in the data
mins_offset=0;
secs_offset=0;
for j=StartFile:EndFile;
    if j<10;
        fname=['s',int2str(specimennumber),'F0000',int2str(j),'.hdr'];
    elseif j>9 && j<100;
        fname=['s',int2str(specimennumber),'F000',int2str(j),'.hdr'];
    elseif j>99 && j<1000;
        fname=['s',int2str(specimennumber),'F00',int2str(j),'.hdr'];
    elseif j>999 && j<10000;
        fname=['s',int2str(specimennumber),'F0',int2str(j),'.hdr'];
    elseif j>9999 && j<100000;
        fname=['s',int2str(specimennumber),'F',int2str(j),'.hdr'];
    else
        fname=['s',int2str(specimennumber),'F',int2str(j),'.hdr'];
    end
    [RunTime,SingleData,Data,Time]=...
        Teac2Matlab(mins_offset,secs_offset,secs_to_read,fname,EndFile);
    TestData=[SingleData,Data,Time];
    DataTimeStamp(j,:)=['',Data,',',Time];
    MaxV(:,j)=max(abs(SingleData),[],2);
    MinV(:,j)=min(abs(SingleData),[],2);
    clear SingleData RunTime TestData
end
Results=[num2str(MaxV(1:totalchannelsread,:))DateTimeStamp];
clear title
t0=clock;
%Max Values from each channel
for i=channelstart:channellend;
```

```

V(i,:)=MaxV(i,:);
Values(i,:)=V(i,:)*channelconversions(i,:);
intervalMaxValues(i,:)=max(Values(i,:));
changefrominitial(i,:)=intervalMaxValues(i,:)-initialvalues(i,:);
end
%Min Values from each channel
for i=5:8
    V2(i,:)=MinV(i,:);
    Values2(i,:)=V2(i,:)*channelconversions(i,:);
    intervalMinValues(i,:)=min(Values(i,:));
    changefrominitial2(i,:)=intervalMinValues(i,:)-initialvalues(i,:);
end
end
%-----
% This section plots the data required
correctionaxis=[0:1:StartFile-2]*0;
xaxis1=[StartFile:1:EndFile];
xaxis=cat(2,correctionaxis,xaxis1);
yaxisplotcorrection=ones(totalchannelsread,length(xaxis));
for i=channelstart:channelend;
    channelfrominitial(i,:)=...
        yaxisplotcorrection(i,:)*changefrominitial(i,:);
    initialvaluesplot(i,:)=yaxisplotcorrection(i,:)*initialvalues(i,:);
    maxlimitplot(i,:)=yaxisplotcorrection(i,:)*maxlimit(i,:);
    minlimitplot(i,:)=yaxisplotcorrection(i,:)*minlimit(i,:);
end
end
%-----
%Plotting Loop for Max Values
abovemax=1.1; %Percentage above Y value
belowmin=.9; %Percentage below min Y value
scrsz=get(0,'ScreenSize');
figure('Position',[0 scrsz(4)*.04scrsz(3)*.5scrsz(4)*.88])
%[distance from left, distance from bottom, width, height]
for i=1.4;
    Ymax(i)=max(values(i,StartFile:EndFile));
    Ymin(i)=min(Values(i,StartFile:EndFile));
    subplot(4,1,i)
    plot(xaxis,Values(i,:),'-k',...)
        xaxis,initialvaluesplot(i,:),'-b','Linewidth',1.5);
    axis([StartFile EndFile belowmin*Ymin(i) abovemax*Ymax(i)]);
end

```

```

Title1L1=['SRCF
Specimen',num2str(specimennumber),':','...'Channel',num2str(i)];
Title1L2=['Start                               Time
num2str((reclenght+recinterval)*StartFile/60+tc),'min End Tlme=',...
num2str((reclenght+recinterval)*EndFile/60+tc),'min'];
title(P{Title1L1;Title1L2});
ylabel('Voltage(V)')
grid;
hold;
legend('Max Values', 'Initial Value','Location','EO');
% set(gca,'Ytick',belowmin*Ymin(i):...
% (abovemax*Ymax(i)-belowmin*Ymin(i)/5:abovemax*Ymax(i));
end

```

APPENDIX B

Outline for RCF test setup procedure

1. Insert rollers.
 - a. Slide the rollers on the roller bracket
 - b. Place the roller locking plates and bolt it down to the shaft
2. Insert specimen.
 - a. Push the loading mechanism outwards.
 - b. Insert the specimen in the chuck.
 - c. Bring in the live centre to support the specimen.
3. Insert eddy current probe.
 - a. Insert the eddy current probe into the probe holder device.
 - b. Set the distance between the probe and the specimen using a feeler guage.
4. Apply loading.
 - a. Switch on the hydraulic power unit.
 - b. Use the pressure regulator to set the pressure to the desired value.
 - c. Switch on the directional valve to the position set to load up the hydraulic cylinders.
5. Fill up the oil tank with transmission oil.
6. Setup eddy current detection device.
 - a. Following settings have to entered before testing into the Defectomat EZ
 - i. Inspection frequency.

- ii. Line Speed.
 - iii. High pass and low pass filter values.
 - iv. Sensitivity.
7. Power on Teac LX-10
 8. Power on personal computer.
 9. Setup LX-Navi program
 - a. Create a folder for all the data to be saved into.
 - b. Open the LX-Navi program.
 - c. Click the new file button in the main window in file drop box menu
 - i. Set the options for the new file
 1. Set the directory to the folder created in a.
 2. Set the file name (ex – s1F).
 3. Set the number of zeroes in the file name.
 4. Check the PC recording system.
 - d. In the main window, click the system button.
 - i. Under the system tab, set the system values.
 1. Set the sampling rate.
 2. Synchronize the LX-Navi clock with the PC clock.
 3. Check slot 1.
 4. Set the number of channels for slot 1.
 - ii. Under the slot1 (PA-8) tab, set the channel values.
 1. Set the calibration value for each channel.
 - I. Channels 1 to 4: 3.16V.

II. Channels 6 and 7: 10V.

- e. Click the trigger button in the setup drop box menu.
 - i. Set the trigger options
 - a. Check the interval check box.
 - b. Set the record time.
 - c. Set the interval time.
 - d. Set the repeat count value.
 - e. Set the start time.

10. Set up monitoring and controlling devices.

- a. Drag the Matlab® files into the directory that the files from the TEAC will be created in.
- b. Turn the control switches on the face of the controllers to off.
- c. Flip the two breakers in the breaker box to power up the motor controllers. Breaker group 13-15-17 and 37-39-41.

11. Acquire initial values.

- a. Open MATLAB®
 - i. Set MATLAB® working directory to the folder where all the files are located.
 - ii. Open the TeatParametersValues file.
 - iii. Edit the values and set them to the current known values, save the file.
 - iv. In the MATLAB® prompt window type type TestParametersValues.

- v. In the MATLAB® prompt window type motorcommand.
 - b. Flip the switches on the front of motor controllers box on to turn on the motors. Let them power up to full speed.
 - c. Determine the initial values by:
 - i. Open the LX-Navi digital readout and visually record max value.
 - ii. Record several files and analyze with T2Mv2Analysis file.
 - 1. If the option is used, a new file must be setup in the LX-Navi.
 - d. Turn the switches off in front of the motor controllers.
 - e. Open the TestParametersValues file and enter initial values.
 - i. Based on the initial values, set the maximum allowable change on each channel.
 - ii. Save the TestParametersValues file.
12. Start the S-RCF tester.
- a. Clear any old data files created in the folder.
 - b. Set the start time in the LX-Navi trigger menu.
 - c. Enter RealTimeDataAnalysis into the Matlab® prompt window and press enter.
 - d. Turn the switches on the front of the motor controllers on.
 - e. Allow the motors to reach full speed
 - f. Monitor the tester for some time to ensure the graphs appear to be reasonable.

Outline for RCF Test Disassembly Procedure

- 1. Stop power to the motors.

- a. Turn the switches on the motor controller box to off, even if the motors are already stopped.
2. Stop the LX-Navi and the Matlab® programs.
 - a. Click the stop button in the LX-Navi to stop further recording.
 - b. To terminate the loop in the program, in the prompt window of Matlab®, hold 'ctrl' and press 'c'.
3. Switch off the Data Recording System.
4. Remove the eddy current probe.
5. Open the cover of the S-RCF tester.
6. Drain the lubricant from the oil tank.
7. Push back the loading mechanism.
8. Remove the specimen.

APPENDIX C

Partslist

Sr. No.	Part Name	Manufacturer	Distributor	Part Number	Qty.	Unit Price	Total Price
1	Base Plate	Tri-Steel	Tri-Steel		1	1200	1200
2	Chuck Shaft	SRS Mfg	SRS Mfg		1	150	150
3	Shaft Drive	SRS Mfg	SRS Mfg		1	200	200
4	Roller Shaft Long	SRS Mfg	SRS Mfg		1	130	130
5	Roller Shaft Short	SRS Mfg	SRS Mfg		1	116	116
6	Roller Plate	SRS Mfg	SRS Mfg		2	37	74
7	Roller Bracket	SRS Mfg	SRS Mfg		2	140	280
8	Roller	SRS Mfg	SRS Mfg		8	68	544
9	Bearing Mount Drive Wall	SRS Mfg	SRS Mfg		1	500	500
10	Rail	SRS Mfg	SRS Mfg		4	75	300
11	Guide Side Top	SRS Mfg	SRS Mfg		4	50	200
12	Guide Centre Top	SRS Mfg	SRS Mfg		2	105	210
13	Guide Side Bottom	SRS Mfg	SRS Mfg		4	110	440
14	Guide Bottom	SRS Mfg	SRS Mfg		2	115	230
15	Bearing Mount Chuck Wall	SRS Mfg	SRS Mfg		1	440	440
16	Drive Bearing Mount	SRS Mfg	SRS Mfg		1	350	350
17	Bearing Mount Chuck	SRS Mfg	SRS Mfg		1	350	350
18	Idler Block	SRS Mfg	SRS Mfg		2	75	150

19	Idler Plate	SRS Mfg	SRS Mfg	2	55	110
20	Idler Sprocket Insert	SRS Mfg	SRS Mfg	2	80	160
21	Idler Bar	SRS Mfg	SRS Mfg	2	35	70
22	Cylinder Rod	SRS Mfg	SRS Mfg	2	70	140
23	Cylinder Mount Vertical	SRS Mfg	SRS Mfg	2	395	790
24	Cylinder Mount Horizontal	SRS Mfg	SRS Mfg	2	340	680
25	Cylinder Mount Base Plate	SRS Mfg	SRS Mfg	2	265	530
26	Chuck Mount	SRS Mfg	SRS Mfg	1	260	260
27	Loading Member	SRS Mfg	SRS Mfg	2	290	580
28	Loadine Bearing Mount Left	SRS Mfg	SRS Mfg	2	200	400
29	Oil Container support 1	SRS Mfg	SRS Mfg	2	85	170
30	Oil Container support 2	SRS Mfg	SRS Mfg	2	85	170
31	Oil Container support 3	SRS Mfg	SRS Mfg	2	85	170
32	Oil Container support 4	SRS Mfg	SRS Mfg	2	85	170
33	Tailstock Base	SRS Mfg	SRS Mfg	1	105	105
34	Tailstock Support	SRS Mfg	SRS Mfg	1	85	85
35	Loading Bearing Mount	SRS Mfg	SRS Mfg	2	175	350
36	Tailstock Block	SRS Mfg	SRS Mfg	1	210	210
37	Oil Container Drive	SRS Mfg	SRS Mfg	1	300	300
38	Oil Container Chuck	SRS Mfg	SRS Mfg	1	300	300
39	Oil Container	SRS Mfg	SRS Mfg	2	240	480

	Cylinder						
	Heat Treatment						
40	Charges	SRS Mfg	SRS Mfg		1	286	286
41	I Beam	Tri-Steel	Tri-Steel		1	200	200
42	Bearings	NTN	Grainger	5ZUK7	8	88	704
43	Seal		Mcmaster	13125K12	4	26	104
44	Hydraulic Cylinder	Parker	Motion Industries	CHD	2	750	1500
45	Pressure Regulator	Parker	Grainger	6PAE4	1	902	902
46	Directional Valve	Prince	Grainger	6W565	1	182	182
47	Assorted Bolts	Fastenal	Fastenal		1	800	800
48	Assorted Hydraulic fittings	Car Quest	Car Quest		1	200	200
Total							16972

APPENDIX D

Parker CHD cylinders

Catalog HY08-1137-5/NA
Cylinder Features

Compact Hydraulic Cylinders
Series CHD

Series CHD Cylinder Features

Primary Seal – polyurethane rod seal with multiple sealing edges is self-compensating and self-relieving to withstand pressure variations and conform to mechanical deflection that may occur.

Piston Rod – Medium carbon steel, hard chrome plated and polished.

Ports – SAE O-ring ports are standard.

OPTIONAL PORTS
NPTF and BSPP ports are also available. Manifold ports are available on mounting styles C & CN.

Secondary Seal – Rod Wiper – wipes clean any oil film adhering to the rod on the extend stroke and cleans the rod on the return stroke.

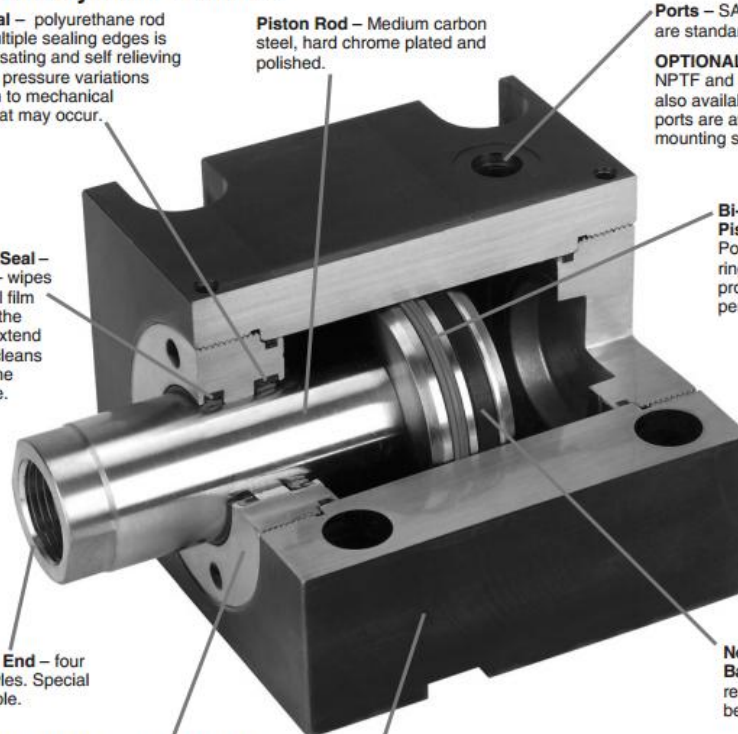
Bi-directional Piston Seal – Polyurethane seal ring with energizer provides leak-free performance.

Piston Rod End – four standard styles. Special ends available.

Non-Metallic Wear Band – improves resistance to bearing loads.

Rod Gland – nodular iron bearing with RoHS compliant zinc plating for corrosion resistance. Optional pilot gland available at no additional cost.

Cylinder Body – steel with black oxide exterior surface treatment.



CHD

Hydraulic power unit

1½- to 15-Gal. AC Power Units

Haldex



No. 4F679



No. 6W644

Note: Recommended motor starters are available on page 304.

½- TO 2-HP, 1½-GAL.

Heavy-duty cast-iron pumps feature quiet 11-tooth hardened steel gears. Aluminum center adapter serves as a port manifold and valve housing with load-holding check and adjustable relief valve. Include standard 1½-gal. oil reservoir; 2½-gal. reservoir is available, see accessories on this page. 9/16-18/#6 SAE outlet and return ports.

1- TO 5-HP, 5- AND 15-GAL.

- D03 manifold units have ¾" (FNPT) cylinder ports, and ½" NPT and ¾" SAE inlet and outlet ports
- D05 manifold units have ½" (FNPT) cylinder ports, and ¾" NPT and SAE inlet and outlet ports

All units come completely assembled with pressure balance pump, filler breather, fluid level gauge with thermometer, pressure gauge, relief valve, and manifold block for mounting single D03 or D05 valve (not included; see page 3846). Manifold is removable for direct pressure and tank (P&T) plumbing. Block includes both NPT and SAE ports.

Reservoir Cap.	HP	Nominal gpm	Max. Pressure psi	Voltage	Phase	Full Load Amps	Recommended Motor Starter	rpm	Manifold Block	L (in.)	W (in.)	H (in.)	Mfr. Model	Item No.	\$ Each
Single-Stage															
1½ gal.	½	0.5	1500	115/230 VAC	1	10.0/4.2-5.0	1H385	1800/1500	—	21	8¼	8¼	1280546	4F678	✓ 678.50
1½ gal.	1	0.5	3000	115/208-230 VAC	1	13.2/6.8-6.6	1H385	1800/1500	—	23	8¼	8¼	1280547	4F679	✓ 761.00
1½ gal.	1	1	1500	115/208-230 VAC	1	13.2/6.8-6.6	1H385	1800/1500	—	23	8¼	8¼	1280548	4F680	✓ 761.00
1½ gal.	1	1	1500	230/460 VAC	3	4.0/2.0	1H412	1800/1500	—	21¼	8¼	8¼	1280551	4F683	✓ 714.00
1½ gal.	1	1.5	1000	115/208-230 VAC	1	13.2/6.8-6.6	1H385	1800/1500	—	23	8¼	8¼	1280549	4F681	✓ 739.00
1½ gal.	1	2	750	115/208-230 VAC	1	13.2/6.8-6.6	1H385	1800/1500	—	23	8¼	8¼	1280550	4F682	✓ 768.00
1½ gal.	1	2	750	230/460 VAC	3	4.0/2.0	1H412	1800/1500	—	21¼	8¼	8¼	1280552	4F684	✓ 700.00
1½ gal.	2	2	1500	230/460 VAC	3	6.0/3.0	1H412	3600	—	21¼	8¼	8¼	1280553	4F685	✓ 732.00
1½ gal.	2	4	750	230/460 VAC	3	6.0/3.0	1H412	3600	—	21¼	8¼	8¼	1280554	4F686	✓ 739.00
5 gal.	1	1	1500	115/230 VAC	1	13.6/6.8	1H385	1800	D03	12	12	24	1400010	6W644	✓ 1,433.00
5 gal.	2	1	3000	115/230 VAC	1	19.0/9.5	1H415	1425/1725	D03	12	14	26	1400034	5PG18	✓ 1,609.00
5 gal.	2	1.5	2000	115/230 VAC	1	19.0/9.5	1H415	1800	D03	12	12	26	1400011	6W645	✓ 1,504.00
5 gal.	2	2	1500	230/460 VAC	3	6.0/3.0	1H412	1800	D03	12	12	25	1400012	6W646	✓ 1,569.00
15 gal.	3	7	600	208-230/460 VAC	3	14.4/12.8/6.4	1H412	3600	D05	25	14	29	1400018	6W636	✓ 1,843.00
15 gal.	5	2.5	3000	208-230/460 VAC	3	15.0/13.6/6.8	1H417	1800	D03	25	14	28	1400013	6W632	✓ 1,794.00
15 gal.	5	3.5	2000	208-230/460 VAC	3	15.0/13.6/6.8	1H417	1800	D03	25	14	28	1400014	6W633	✓ 1,895.00
15 gal.	5	4.5	1500	208-230/460 VAC	3	15.0/13.6/6.8	1H417	1800	D03	25	14	28	1400015	6W634	✓ 1,857.00
15 gal.	5	5	1250	208-230/460 VAC	3	15.0/13.6/6.8	1H417	1800	D03	25	14	28	1400016	6W635	✓ 1,815.00
15 gal.	5	7	1000	230/460 VAC	3	8.0/4.0	1H417	3600	D05	25	14	25	1400017	6W637	✓ 1,884.00
15 gal.	5	9	750	208-230/460 VAC	3	14.4/12.8/6.4	1H417	3600	D05	25	14	29	1400020	6W639	✓ 1,930.00
15 gal.	5	11	600	208-230/460 VAC	3	14.4/12.8/6.4	1H417	3600	D05	25	14	29	1400022	6W641	✓ 1,911.00
2-Stage															
15 gal.	3	11.0/2.8	250/1500	230/460 VAC	3	8.0/4.0	1H417	3600	D05	25	14	26	1400023	6W642	✓ 1,912.00
15 gal.	5	11.0/2.8	450/2400	230/460 VAC	3	8.0/4.0	1H417	3600	D05	25	14	29	1400035	5PG19	✓ 1,976.00
15 gal.	5	16.0/3.8	250/2000	230/460 VAC	3	14.41/12.8/6.4	1H417	3600	D05	25	14	29	1400024	6W643	✓ 1,946.00

Directional Valve

Monoblock Valves

- Load checks provided on all spools (except No. 1A967)
- All valves have direct-acting relief valves

Single-spool valves are 3-position and tandem center, 2- and 3-spool valves have a float spool. No. 1A967 has a pressure detent release preset at 1200 psi. Nos. 6X845, 4HL36, 4HL37, 6W566, and 4HL32 can be converted to closed center or to power beyond operation; No. 6W565 can be converted to closed center only.



Prince

Spool Action	Ways	Spools	Inlet/Outlet Port Size NPT (in.)	Work Port Size NPT (in.)	Capacity gpm	Factory Relief Setting	Relief Range psi	Max. psi	Mfr. Model	Item No.	\$ Each
Spring Center To Neutral	4	1	¾	½	16	1500 psi @ 12 GPM	1000 to 2750	3000	RD2555T4ESA1	6XB44	✓ 183.50
Spring Center To Neutral	4	1	¾	½	30	2000 psi @ 10 GPM	1500 to 3000	3000	RDS12CASA4B1	6XB45	†✓ 248.25
3 Position Detent	4	1	¾	½	20	1500 psi @ 12 GPM	1000 to 2750	3000	RD2575T4EDA1	6W565	†✓ 176.25
3 Position Detent	4	1	¾	½	30	2000 psi @ 10 GPM	1500 to 3000	3000	RDS12CCSA4B1	4HL36	†✓ 267.25
Spring Center To Neutral	4	1	¾	½	25	2250 psi @ 3 GPM	1000 to 2750	2750	LS3000-1	1A967	✓ 179.75
Spring Center To Neutral	3	1	¾	½	30	2000 psi @ 10 GPM	1500 to 3000	3000	RDS12AASA4B1	4HL37	†✓ 261.75
No. 1: Spring Center To Neutral and 4th Position Detent. No. 2: Spring Center To Neutral	4	2	¾	½	25	2000 psi @ 10 GPM	1500 to 3000	3000	RD522GGA5A4B1	6W566	†✓ 380.25
No. 1: Spring Center To Neutral and 4th Position Detent. No. 2 and No. 3: Spring Center To Neutral	4	3	¾	½	25	2000 psi @ 10 GPM	1500 to 3000	3000	RDS32GCCGA5A4B1	4HL32	†✓ 520.00

* Power beyond requires Prince Number 660312004 plug. † Closed Center requires Prince Number 660312005 plug. ‡ Closed center requires Prince Number 200018002. Repair parts can be ordered from your local Grainger branch.

Pressure regulator

Relief Valves

Control maximum pressure within a hydraulic circuit. No. 6X843 is designed for full flow with low pressure drop and constructed of high-strength steel bar stock body with replaceable heat-treated seat.

Nos. 4BA48 to 4BA50 have 2-stage balanced piston design, providing fast response and minimizing pressure override.

No. 4HL34 is a differential poppet inline relief which has a minimum variation between cracking and full flow pressures.

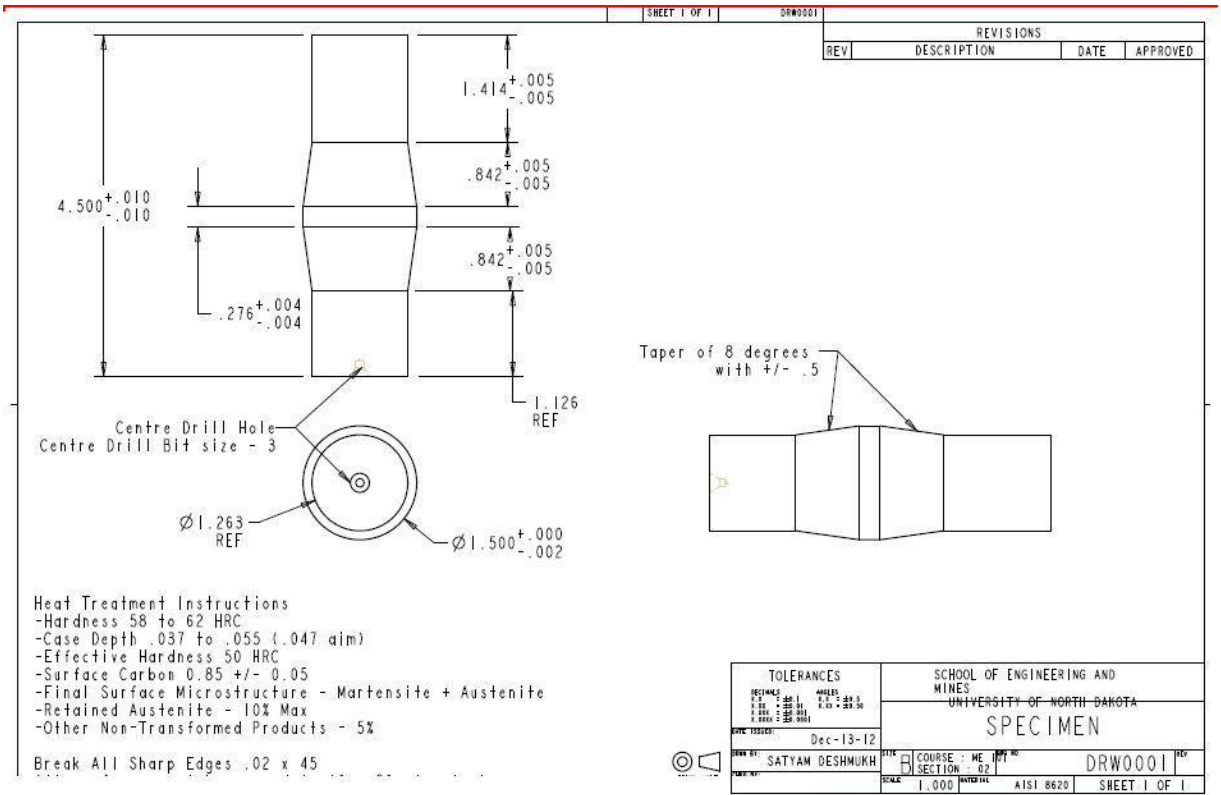
No. 4HL35 is a double differential poppet relief that is used in systems that require cross-over relief protection such as a hydraulic motor.

Item	Port Size	Max. Flow	Pressure Range (psi)	Brand	Mfr. Model	Item No.	\$ Each
Single							
Relief Valve	1/2" NPT	16 GPM	1000 to 2500	Prince	RD1850H	6X843 ✓	71.05
Inline Relief Valve	3/4" NPT	30 GPM	1500 to 3000	Prince	RV-2H	4HL34 ✓	69.25
Adjustable Relief Valve	7/8-14 UNF-2B	45 GPM	125 to 1000	Vickers	CS-03-B50	4BA48 ✓	446.25
Adjustable Relief Valve	7/8-14 UNF-2B	45 GPM	500 to 2000	Vickers	CS-03-C50	4BA49 ✓	446.25
Adjustable Relief Valve	7/8-14 UNF-2B	45 GPM	1500 to 3000	Vickers	CS-03-F50	4BA50 ✓	446.25
Hydraulic Valve	SAE #12	53 GPM	100 to 1532	Parker	R4V065B110A1	6PAE3 ✓	863.50
Hydraulic Valve	SAE #12	53 GPM	100 to 3045	Parker	R4V065B310A1	6PAE4 ✓	863.50
Hydraulic Valve	SAE #12	53 GPM	100 to 5075	Parker	R4V065B510A1	6PAE5 ✓	863.50
Double							
Double Relief Valve	3/4" NPT	30 GPM	1500 to 3000	Prince	DRV-2HH	4HL35 ✓	123.00

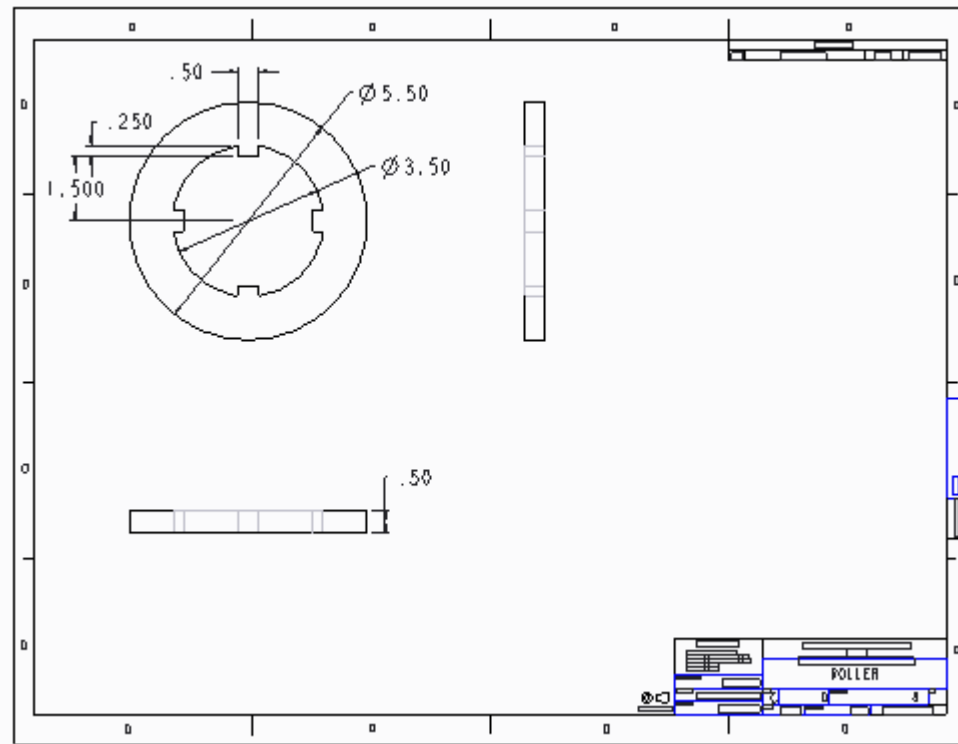


APPENDIX E

Specifications of the specimen



Specifications of the rollers



BIBLIOGRAPHY

- [1] Ralph I. Stephens, R.I. Fatemi, A. Stephens, R.R., & Fuchs, H.O. (2001). Metal Fatigue in Engineering 2nd edition. New York, NY: John Wiley & Sons Inc.
- [2] ASTM Subcommittee E08.02. (2000). Standard Terminology Relating to Fatigue and Fracture. (Vol. 03.01, pp. 1034). Testing ASTM Designation E1823, West Conshohocken, PA: ASTM.
- [3] ASM International Handbook Committee. (2002). ASM Handbook Volume 11: Failure Analysis and Prevention. Materials Park, OH: ASM International.
- [4] Hoffmann, G., & Jandeska, W. (2007, January/ February). Effects on Rolling Contact Fatigue Performance. GEARTECHNOLOGY, 42-42.
- [5] UL Health and Safety Executive (2002) Hartfeild Derailment Investigation, Interim Recommendations of The Investigation Board, <http://www.hse.gov.uk/railways/hatfeild/investigationb1.pdf>, August 2002
- [6] Kapoor A., Fletcher D., Franklin F. (July 2006). Management and Understanding of Rolling Contact Fatigue. Literature Survey.
- [7] Lipp, K., & Hoffman, G. (2003). Design for Rolling Contact Fatigue. International Journal of Powder Metal, 39(1), 33-46
- [8] Deng, G., T., & Kato, M. (2002). Surface Temperature Calculation and its Application to Surface Fatigue Strenght Evaluation. Journal of Mechanical Design, 124, 805-812
- [9] Hoffman, G. & Rice, J.A. (2005). Initiation and Propogation of Cracks in Wrought and Sintered Steels during Rolling Contact Fatigue. Advances in Powder Metallurgy & Particulate Materials, 3(3), Part 10 176-200.
- [10] Dvorak G., (2007). Development of a Sliding-Rolling Contact Fatigue Tester. Grand Forks, ND
- [11] U.S. Tsubaki Sprocket Catalog Retrieved from www.ustsubaki.com

- [12] Parker Hydraulic Cylinder. Retrieve Jan 10 2011, from Parker Catalog. Online <http://www.parker.com/portal/site/PARKER/menuitem>
- [13] Haldex Banded Power Unit. Retrieved Jan 12 2011. Retrieved from Grainger website. Online. [http://www.grainger.com/Grainger/HALDEX-BARNES Hydraulic-AC-Power-Unit](http://www.grainger.com/Grainger/HALDEX-BARNES-Hydraulic-AC-Power-Unit)
- [14] AISI 1144 Stress Proof Steel. Retrieved Dec. 21 2010, from Niagara Lasalle website. <http://www.niagaralasalle.com/product-stressproof.html>
- [15] Beardmore, R. (2007). Coefficient of Rolling Friction. Retrieved on December 12 2010 from RoyMech Index Page. Online. http://www.roytech.co.uk/Useful_Tables/Tribology/co_of_frict.htm
- [16] Spider Couplers. Retrieved Jan 24 2011. Retrieved from Grainger. Online. <http://www.mcmaster.com/#spider-couplings/=l8s6ox>
- [17] Chuck. Retrieved Jan 15 2011. Catalog retrieved from Buck Chuck company. Online <http://www.buckchuckusa.com/products/manual-chucks-at-sc-3jaw.html>
- [18] Campbell, Sylvester J. (1987). Solid-State AC Motor Controls. New York: Marcel Dekker, Inc.. pp. 79–189.
- [19] Juvinall, R., Marshek, K., R.I. (2001). Fundamentals of Machine Component Design 5th edition. New York, NY: John Wiley & Sons Inc.
- [20] Black-Oxide Alloy Steel Socket Head Cap Screws. Retrieved December 24 2010, from McMaster-Carr Catalog [http://www.mcmaster.com/#socket head-cap-screws/=l8mzn5](http://www.mcmaster.com/#socket-head-cap-screws/=l8mzn5)
- [21] Larson, B.F. (n.d.). Introduction to Eddy Current Testing. Retrieved May 2010 from NDT Resource Centre. Online. <http://www.ndt-ed.org/EducationResources/CommunityCollege/EddyCurrents>
- [22] Harkins, W. (1999). NASA-STD-5007:LLIS-0760 Eddy Current Testing of Aerospace Materials. Retrieved May 25 2010, from NASA Technical Standards Program. Online <http://www.nasa.gov/offices/oce/llis/0760.html>
- [23] Cartz, L. (1995). Nondestructive Testing: Radiography, Ultrasonics, Liquid Penetrant, Magnetic Particle, Eddy Current, Materials Park, OH: ASM International.

- [24] Baldev, R., Jayakumar, T., & Thavasimuthu, M. (2002). Practical Non Destructive Testing 2nd Edition. Cambridge, England: Woodhead Publishing Limited.
- [25] Foester Instruments Incorporated. (2003.). Defectomat: Eddy Current Testing Equipment. Retrieved May 23 2010, from Foester Instruments Incorporated. Online. <http://www.foestergroup.com/NDT/defectomat.html>
- [26] Hoffmann, G., & Jandeska, W. (2007, March/April). Effects on Rolling Contact Fatigue Performance – Part II. GEARTECHNOLOGY, 42-51.